Deep Artifact Reduction for CT

Marc Kachelrieß

German Cancer Research Center (DKFZ)
Heidelberg, Germany
www.dkfz.de/ct

DEUTSCHES
KREBSFORSCHUNGSZENTRUM
IN DER HELMHOLTZ-GEMEINSCHAFT

Latent Space Reconstruction

LSR

Original

Truncated

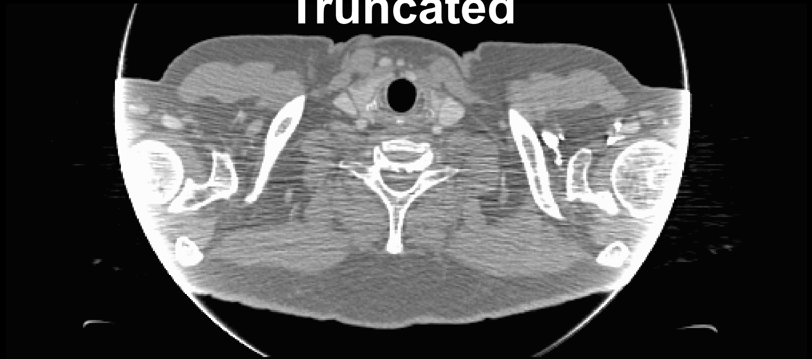

ADT-corrected

ADT-corrected (clipped)

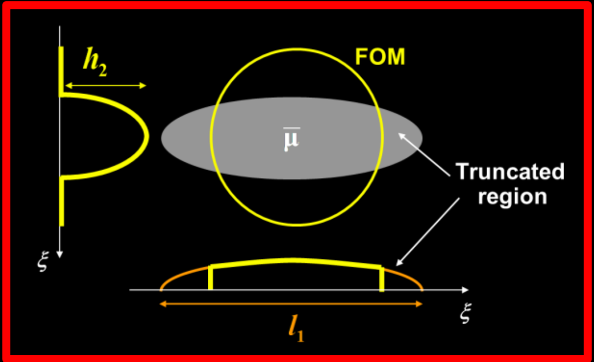

C = 0 HU, W = 1000 HU

K. Sourbelle, M. Kachelrieß, and W.A. Kalender. Reconstruction from truncated projections in CT using adaptive detruncation (ADT). Eur Rad 15:1008–1014, 2005.

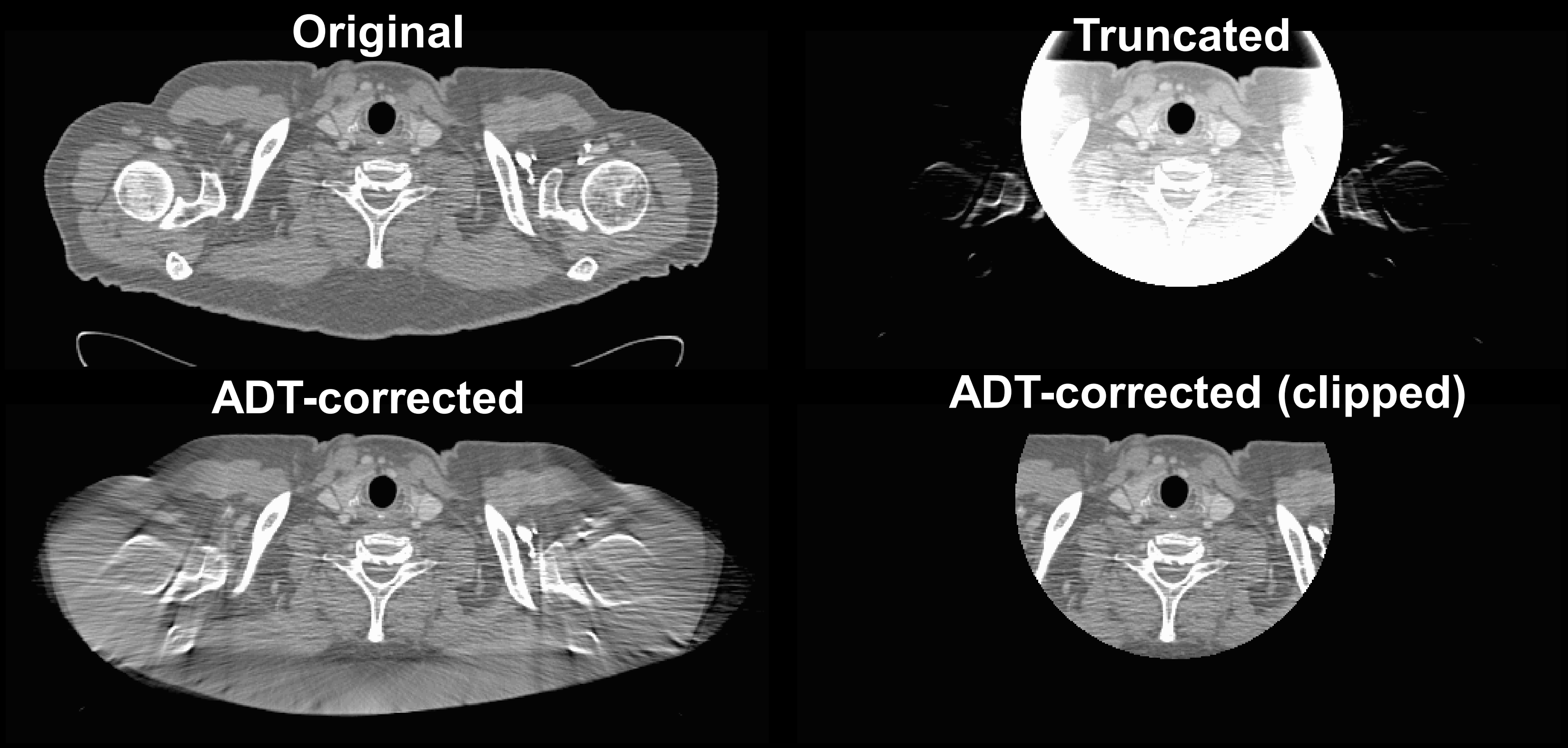

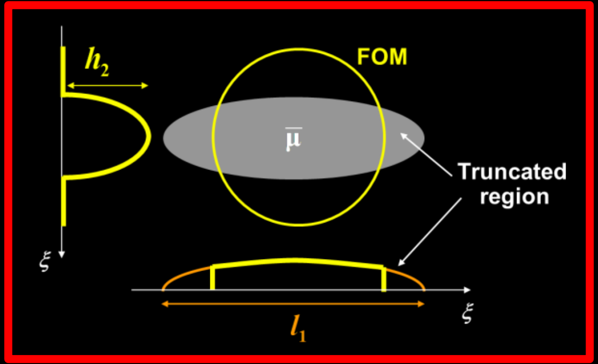

C = 0 HU, W = 1000 HU

K. Sourbelle, M. Kachelrieß, and W.A. Kalender. Reconstruction from truncated projections in CT using adaptive detruncation (ADT). Eur Rad 15:1008–1014, 2005.

Latent Space Reconstruction (LSR)

- Missing data yields ill-posed problems.
- CT examples for missing data
  - Truncation (lateral, longitudinal, …)
  - Limited angle
  - Metal artifacts
  - Longitudinal FOM extension
  - Sparseness artifacts
  - …
- Generative models have the ability to generate CT images or volumes from a low dimensional latent space.
- LSR: Find latent space vector *z* such that the decoded data (images, volumes, sinograms, …) match with the measured data.

VAE Data and Training

- **Data:**
  - Clinical data acquired with a Siemens Somatom Force CT
  - 85 adult patient scans
  - 0.6 mm slice thickness and 0.69 to 0.98 mm axial voxel spacing
  - Randomly split into training, validation and testing (70:15:15)
- **Training:**
  - Trained for 150 epochs
  - Learning rate 0.001
  - Adam optimizer
  - Hybrid loss function consisting of VAE loss, perceptual loss and WGAN generator loss

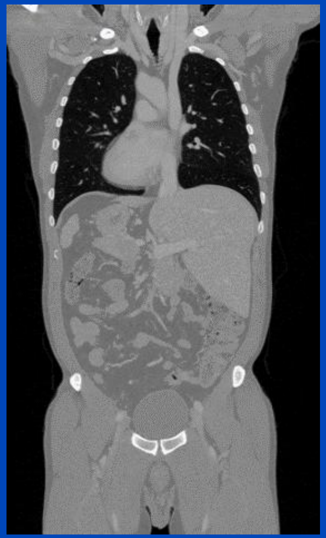

Coronal

Sagittal

$$L = L_{\text{pixel-wise}} + \beta\, L_{\text{Kullback–Leibler}} + \gamma\, L_{\text{perc}} + \delta\, L_{\text{WGAN}}$$

A. Kabelac, E. Eulig, J. Maier, M. Hammermann, M. Knaup and M. Kachelrieß. Latent space reconstruction for missing data problems in CT. Med. Phys. 52(7):e17910, July 2025.

LSR for Detruncation

- Train a VAE on very many untruncated CT images f_n

$$\theta = \arg\min_{\theta} \sum_n \| D(\mathcal{N}(E(f_n(\boldsymbol{r})))) - f_n(\boldsymbol{r}) \|$$

- Find latent space point z to best match the truncated projections p

$$z = \arg\min_{z} \| \mathsf{X} D(z) - p \|$$

- Forward project $D(z)$ and use the resulting rawdata to extrapolate the measured rawdata.
- Do a final image reconstruction of the detruncated sinogram.

Network output is not seen by the reader!

Search in Latent Space

- **Optimization of latent space vector in projection domain**

$$z = \arg\min_{z} \| X D(z) - p \|_{15\ \mathrm{cm}}$$

- **Video showing intermediate images of selected iteration steps.**

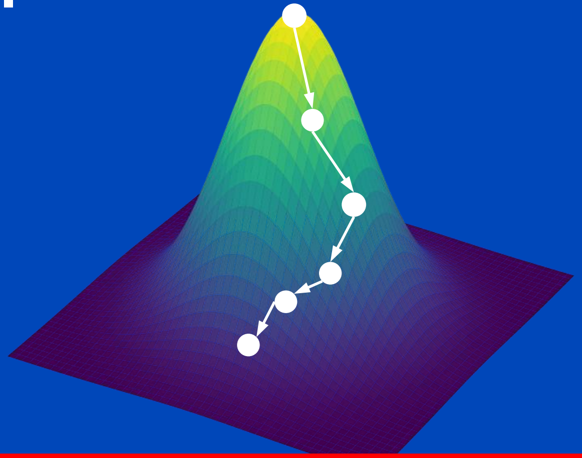

Network output is not seen by the reader!

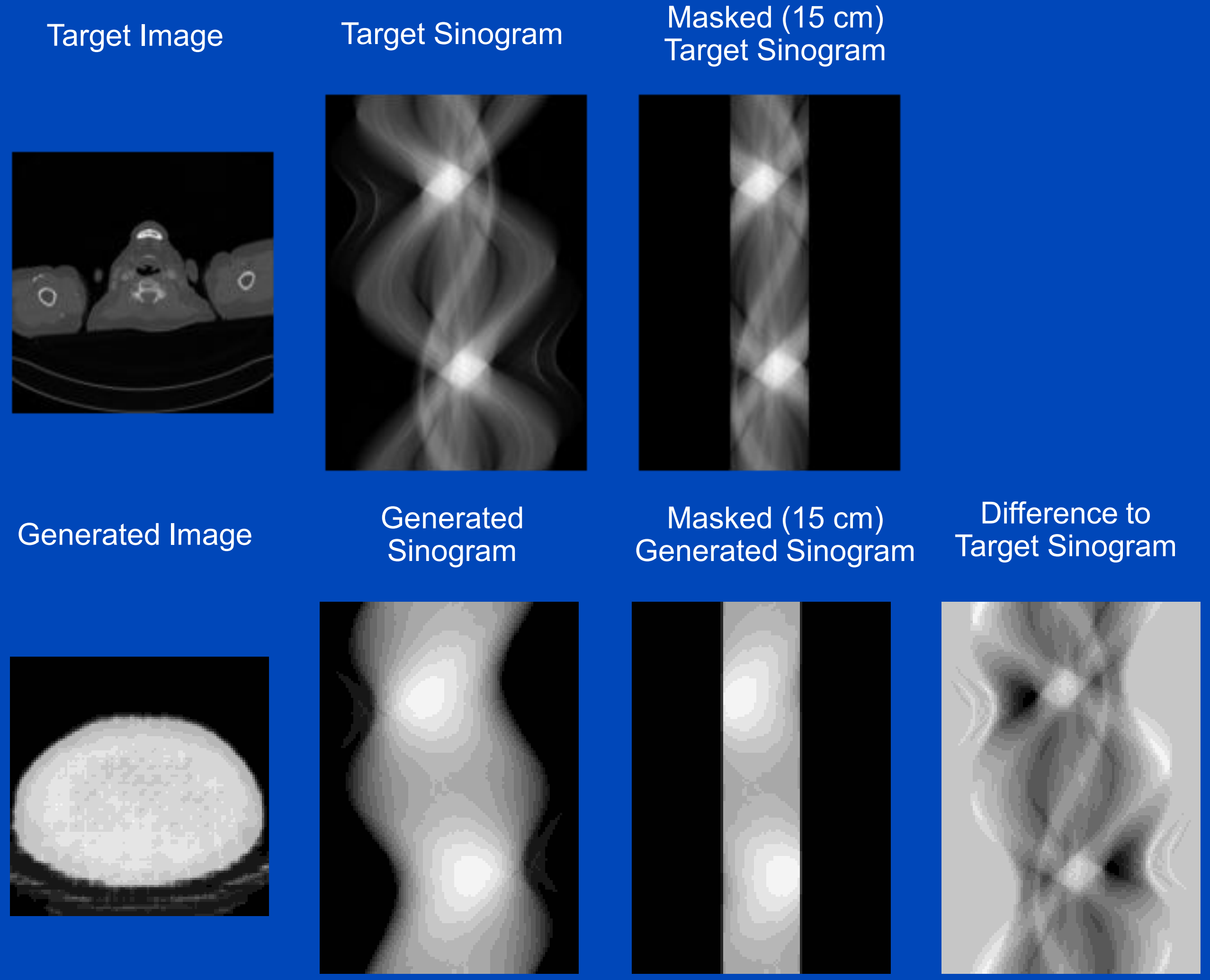

A. Kabelac, E. Eulig, J. Maier, M. Hammermann, M. Knaup and M. Kachelrieß. Latent space reconstruction for missing data problems in CT. Med. Phys. 52(7):e17910, July 2025.

Reference Methods
U-Net-Based Sinogram Extension

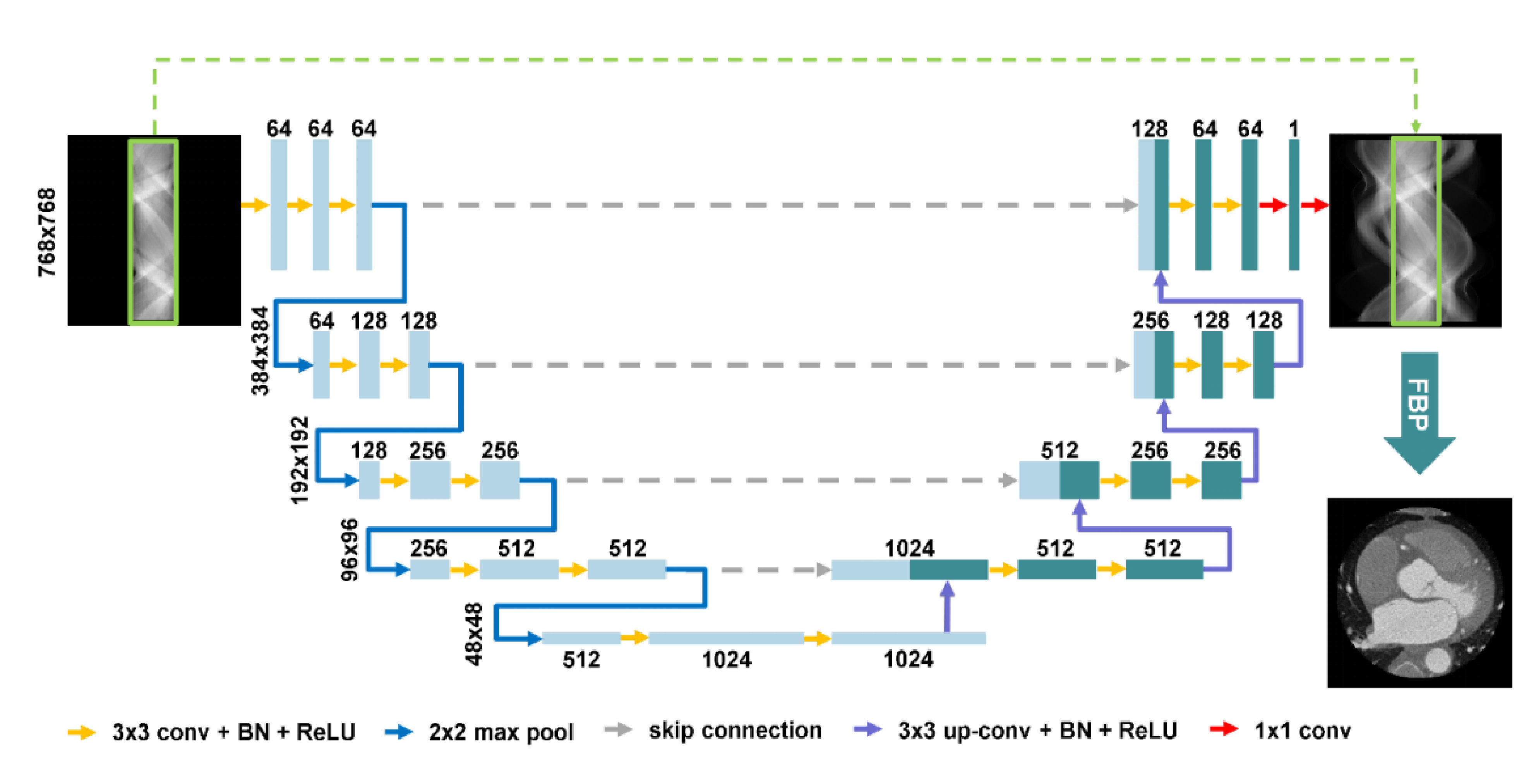

J. HJ. Ketola, et al., Deep learning-based sinogram extension method for interior computed tomography, Medical Imaging: Physics of Medical Imaging. Vol. 11595. International Society for Optics and Photonics (2021)

Results

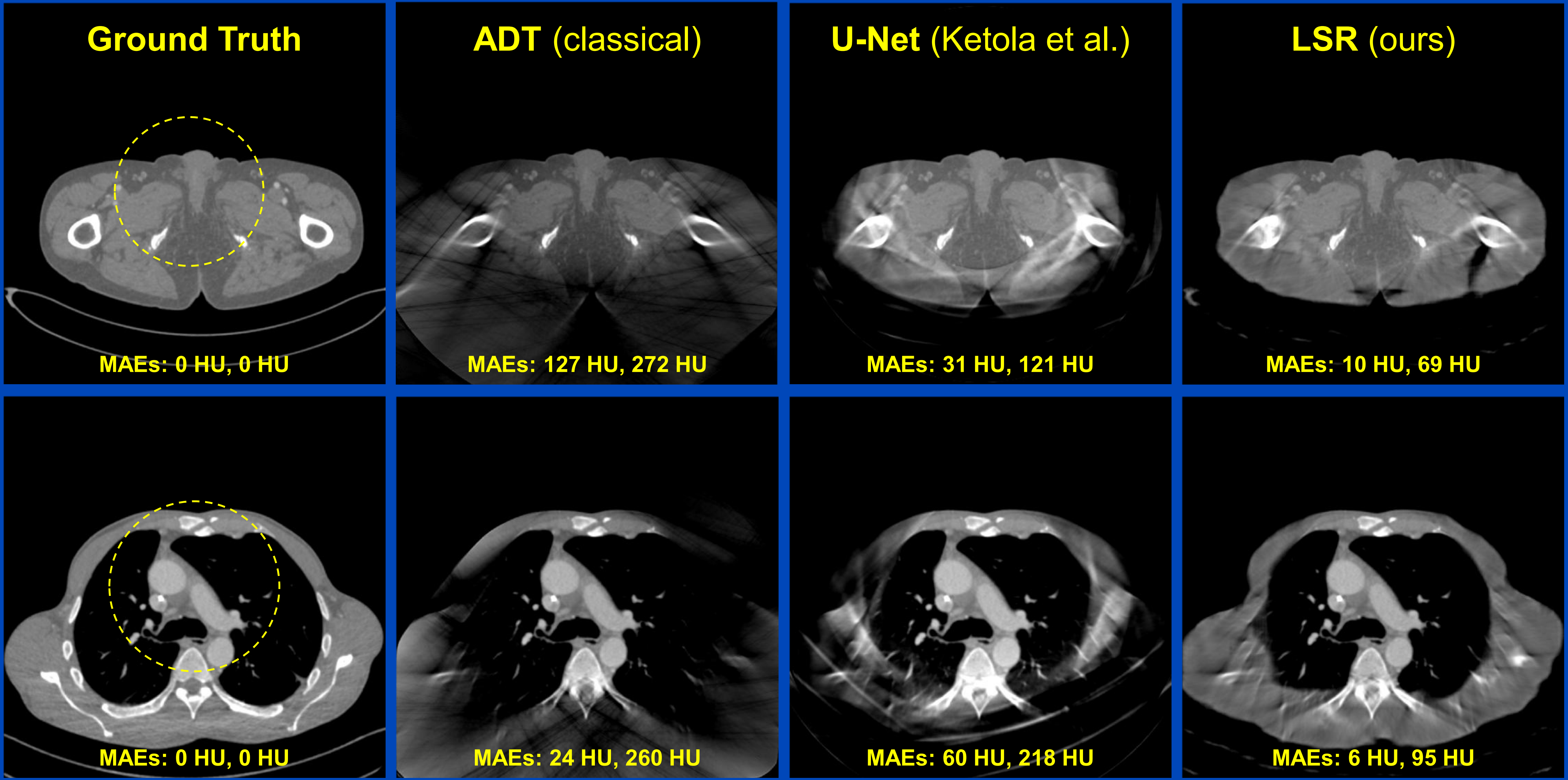

C = 50 HU, W = 1200 HU

Noise-Augmented Deep Denoising

NADD

Noise-Augmented Deep Denoising of CT (NADD)

Gernot Kristof, Achim Byl, Elias Eulig, and Marc Kachelrieß

Abstract—**Denoising low dose CT images can have great advantages for the aim of minimizing patient risk, as it can help lower the effective dose to the patient, while providing constant image quality. Conventional deep denoising algorithms cannot handle the correlation between neighboring pixels or voxels, because the noise structure in CT is a resultant of the global attenuation properties of the patient and because the receptive field of denoising approaches is rather small. In this work additional noise realizations were generated, reconstructed, and used as additional input into a denoising network to guide the denoising process. The network was compared to a similar network, without additional noise augmentation. It was shown, that the noise-augmented deep denoising network outperformed the conventional denoising network. Due to the additional in-**

to 2D images but will be extended to 3D volumes in the near future.

II. Method

The idea of this project is to generate, by noise injection into the rawdata followed by image reconstruction, a multitude of new noise realizations $h_c(\boldsymbol{r})$ of the CT image $g(\boldsymbol{r})$ that is to be denoised. Here we use $C = 10$ noise realizations. These are input to the NADD network, together with the original CT image that is to be denoised. With these ten additional input channels NADD can learn about the noise correlation

Images and Noise Only Images

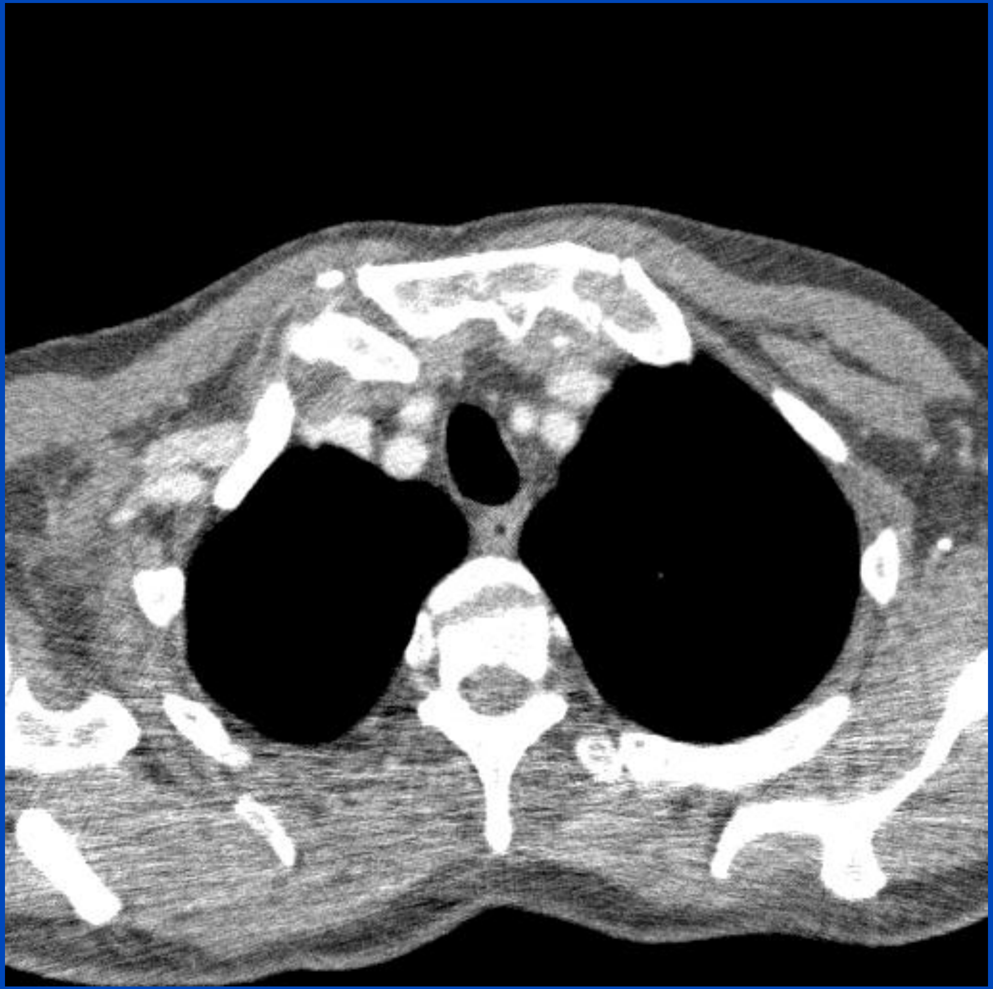

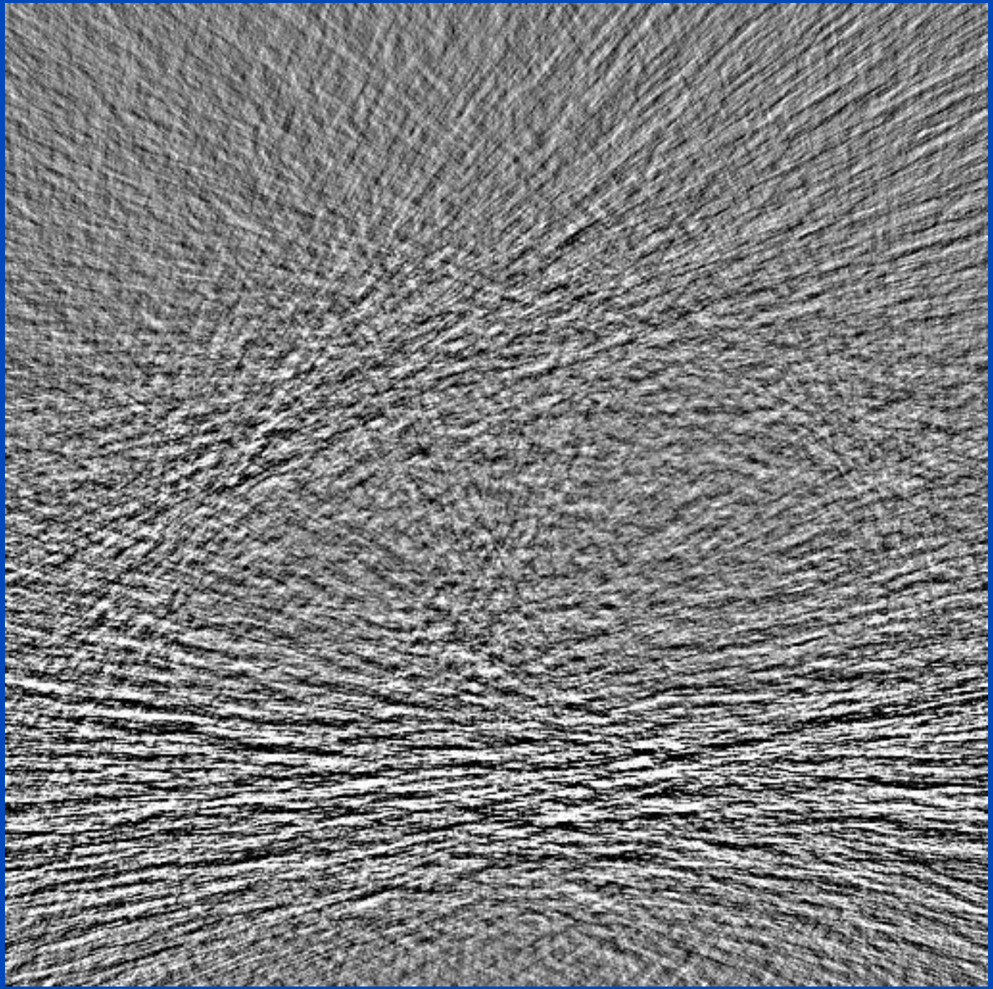

C = 0 HU, *W* = 600 HU

C = 0 HU, *W* = 150 HU

Images and Noise Only Images

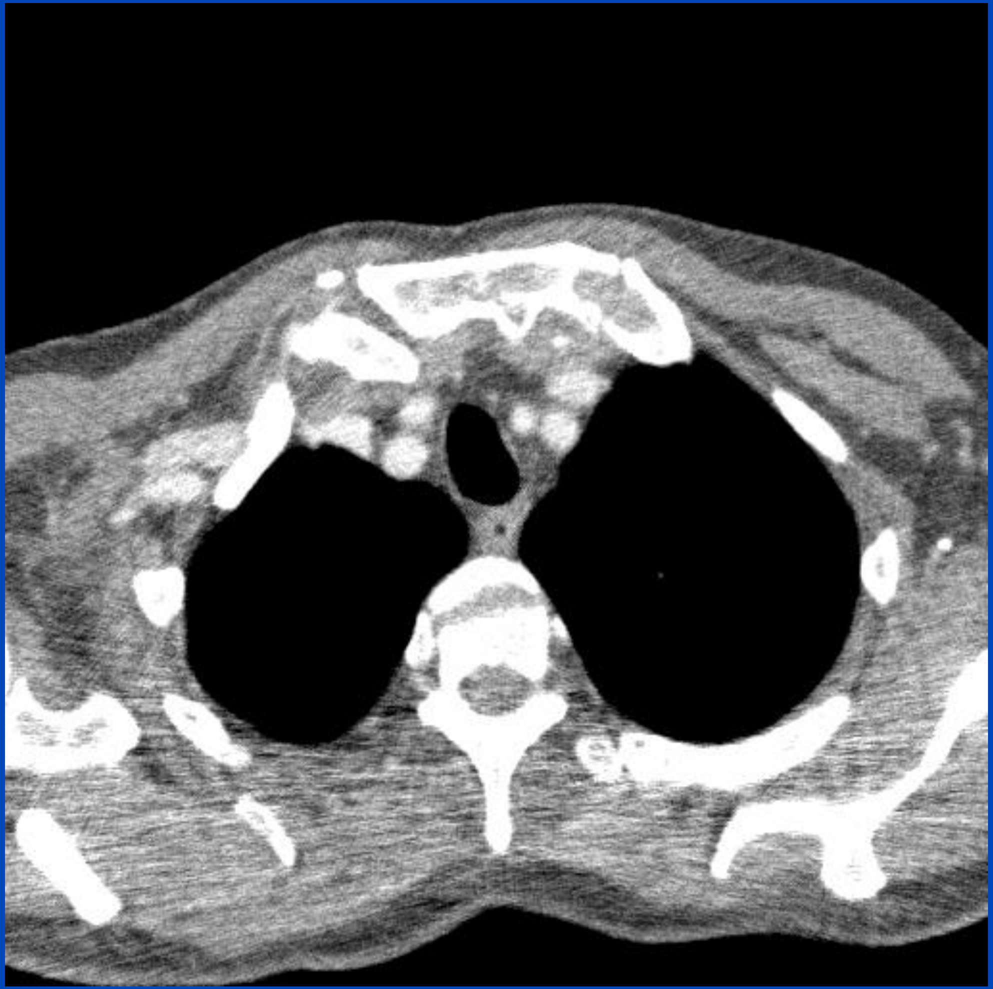

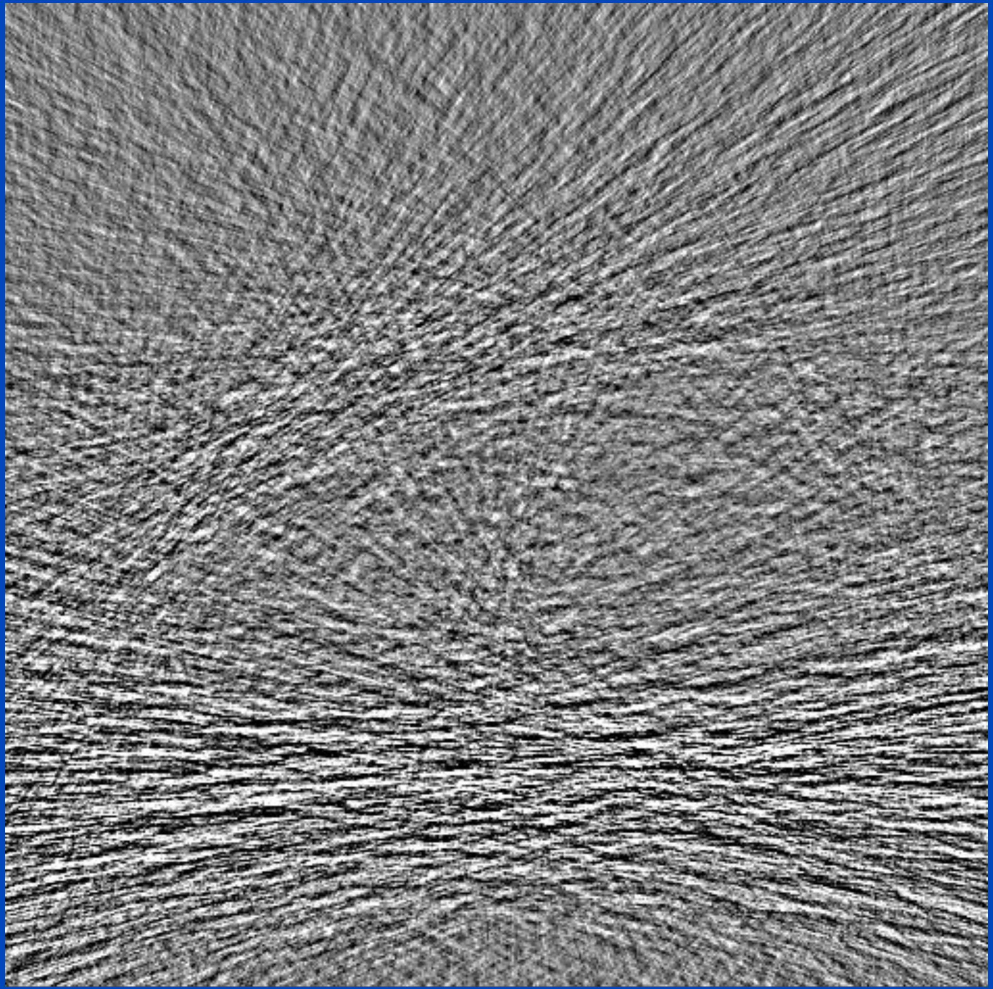

C = 0 HU, *W* = 600 HU

C = 0 HU, *W* = 150 HU

Images and Noise Only Images

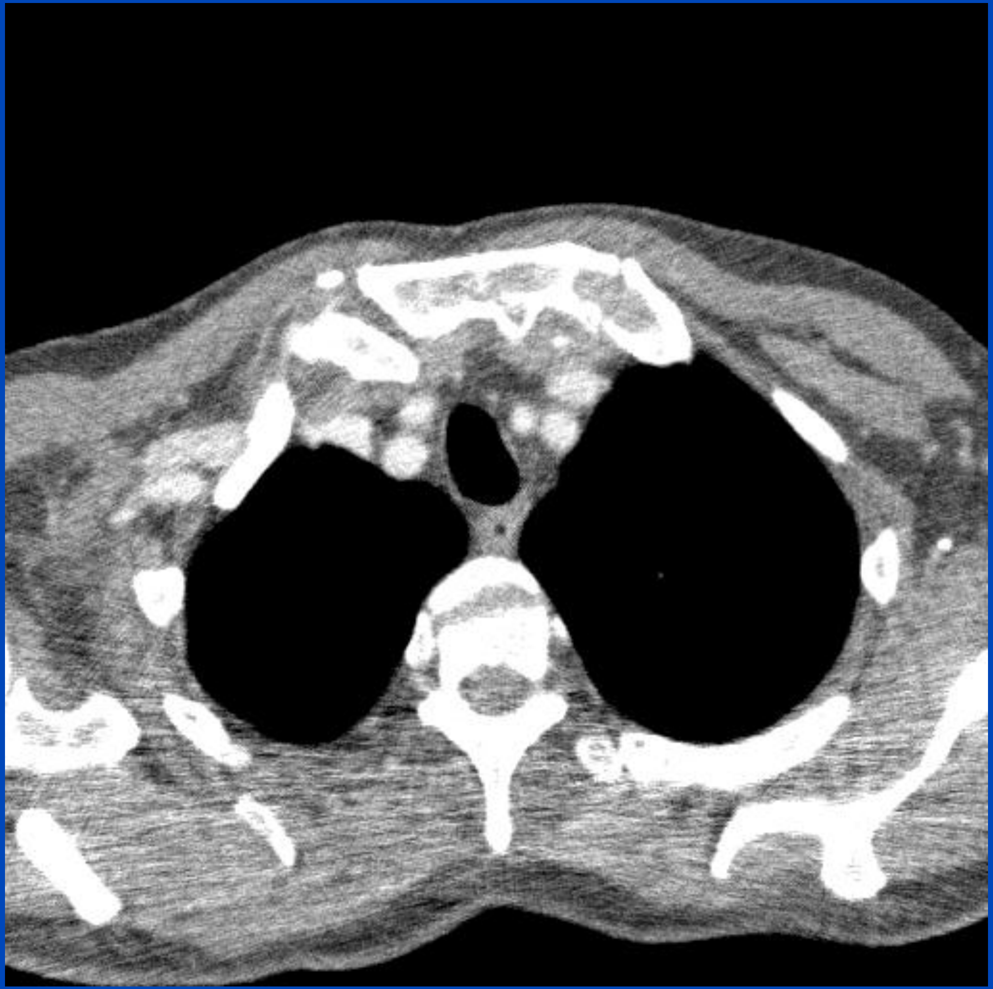

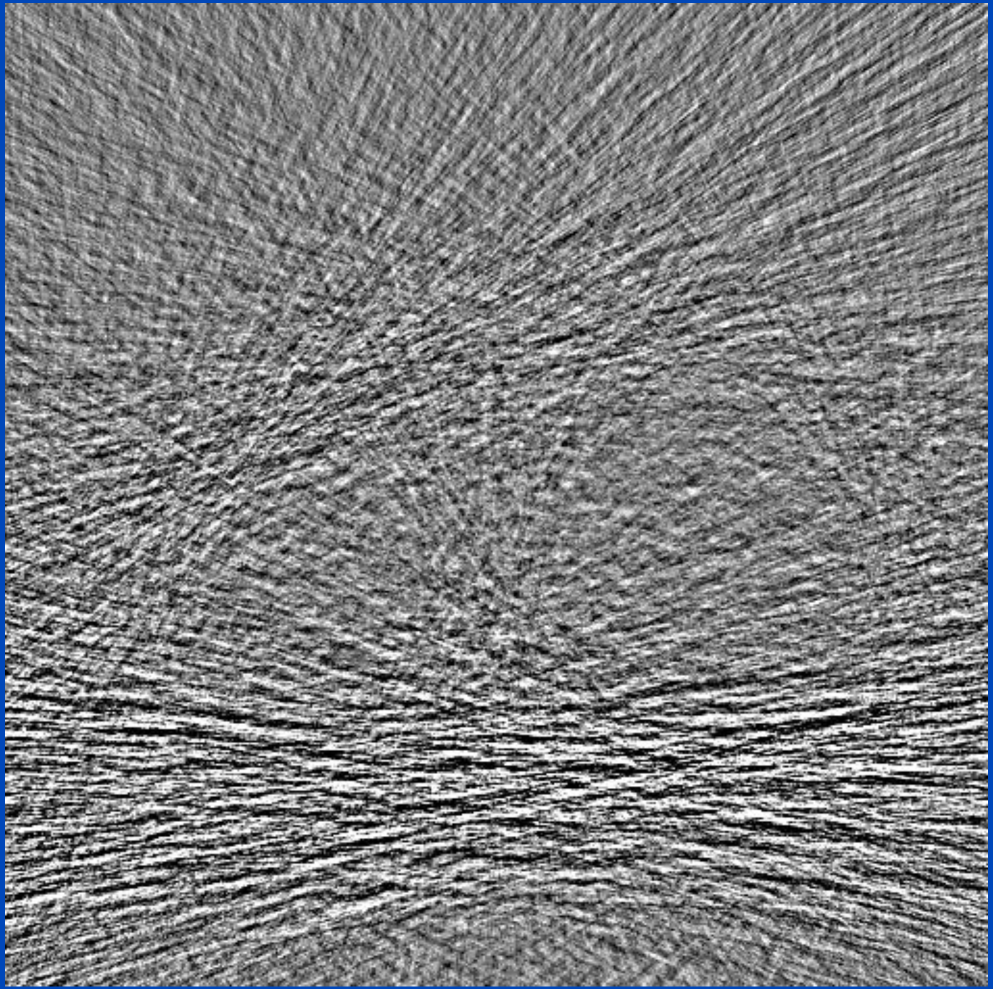

C = 0 HU, *W* = 600 HU

C = 0 HU, *W* = 150 HU

NADD: Background, Aim and Idea

NADD = Noise-augmented deep denoising

- **Background:** CT noise is strongly correlated between pixels. The correlation depends on the patient's attenuation properties and on the tube current curve that was used to generate the images.
- **Aim:** To find out whether noise reduction networks in CT benefit from seeing more than one noise realization.
- **Idea:** Generate, by rawdata noise injection and reconstruction, several noise realizations and provide them to <u>existing</u> denoising networks in addition to the noisy image.

NADD = 1 measurement
+ 10 simulated noise realizations
+ a denoising network

G. Kristof, E. Eulig, and M. Kachelrieß. Noise-Augmented Deep Denoising:
A Method to Boost CT Image Denoising Networks. Med. Phys. 52(10):e18121, October 2025.

Low Dose, Std Dose and all 10 Noise Only Realizations

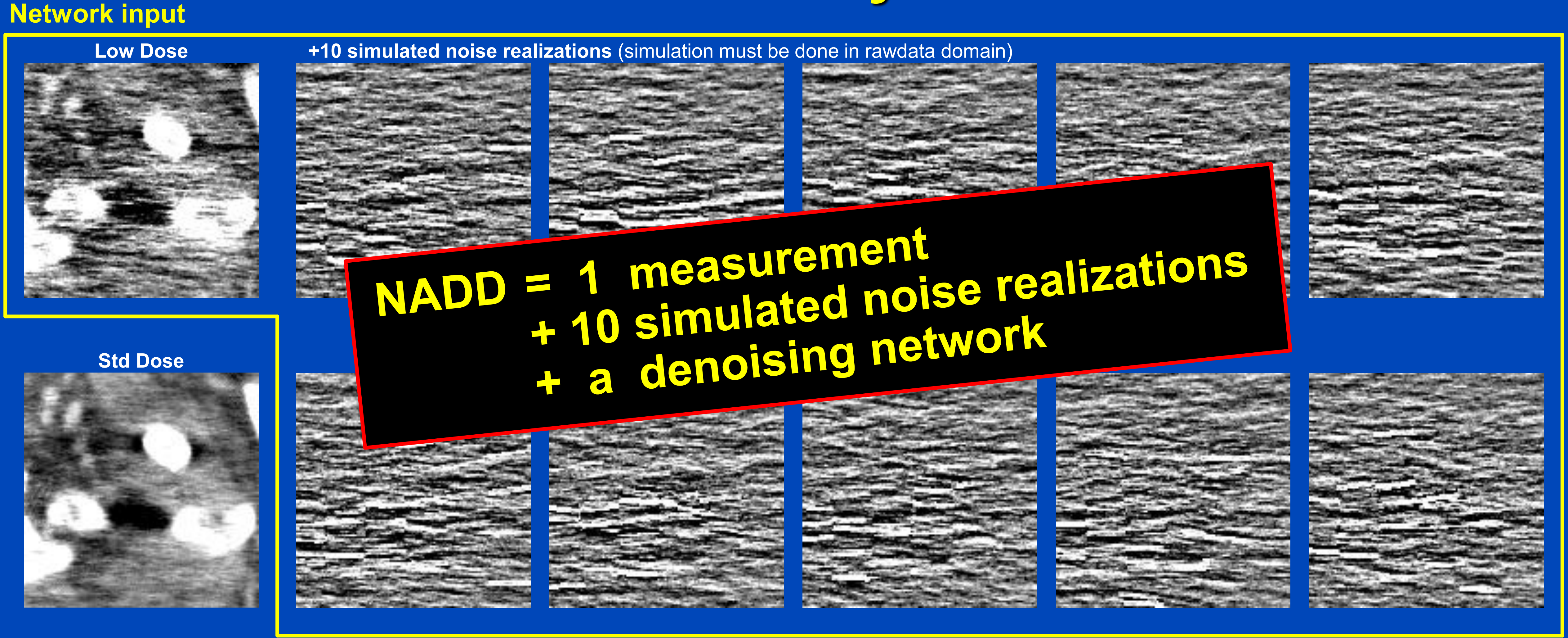

CT Images: C = 0 HU, W = 600 HU. Noise only images: C = 0 HU, W = 550 HU.

G. Kristof, E. Eulig, and M. Kachelrieß. Noise-Augmented Deep Denoising: A Method to Boost CT Image Denoising Networks. Med. Phys. 52(10):e18121, October 2025.

Noise Reduction Networks

- We use a couple of popular noise reduction networks
  - CNN10[1]
  - ResNet[2]
  - WGAN-VGG[3]
- We adapt these networks to the case of 1+*N* input images
  - 1 image to be denoised
  - *N* noise-only images
- We mainly consider the cases $N = 0$ and $N = 10$ in the following.
- We will denote the method and the number *N* of additional noise-only realizations as following: Method_{+N}
  - For example, CNN10_{+10} will indicate the CNN10 method with 10 additional noise realizations as input.

In the results slides: **Low Dose = 10% or 50% of Std Dose**

[1]H. Chen et al. Low-dose CT denoising with convolutional neural network. International Symposium on Biomedical Imaging (ISBI 2017):143-146, 2017.
[2]A. D. Missert et al. Noise subtraction for low-dose CT images using a deep convolutional neural network. Proc. of the Fifth Int. Conf. on Image Formation in X-Ray CT:399-402, 2018
[3]Q. Yanget al. Low-dose CT image denoising using a generative adversarial network with Wasserstein distance and perceptual loss. IEEE TMI 37(6):1348-1357, June 2018.

Network Architectures – $\mathrm{CNN10}_{+N}$

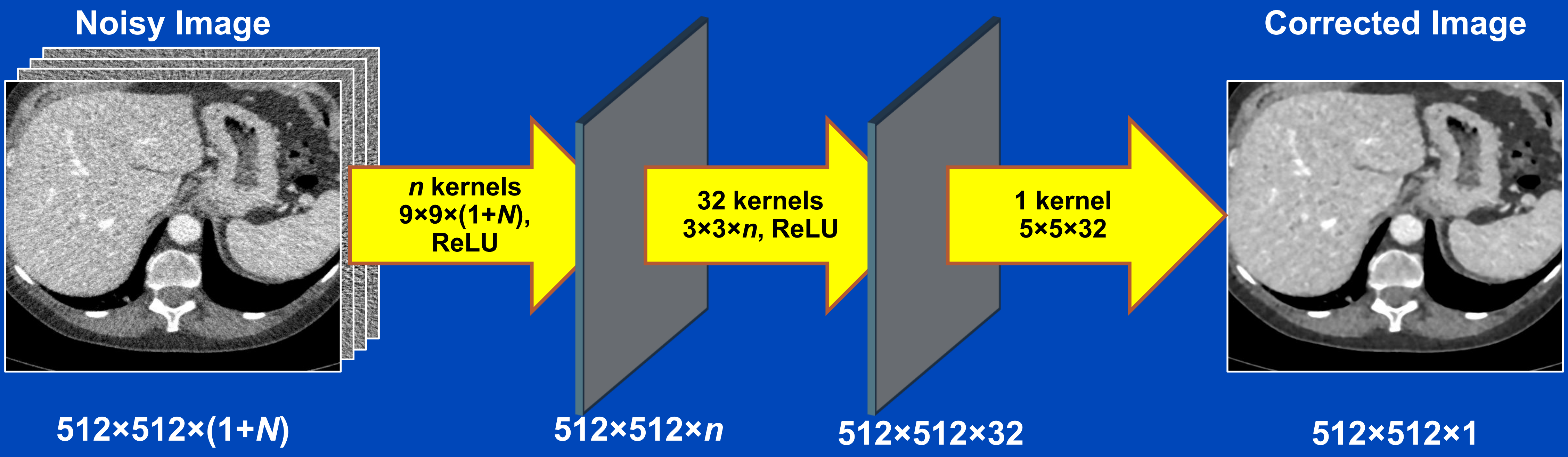

[1] H. Chen *et al.*, "Low-dose CT denoising with convolutional neural network," *2017 IEEE 14th International Symposium on Biomedical Imaging (ISBI 2017)*, 2017, pp. 143-146, doi: 10.1109/ISBI.2017.7950488.

Network Architectures – ResNet

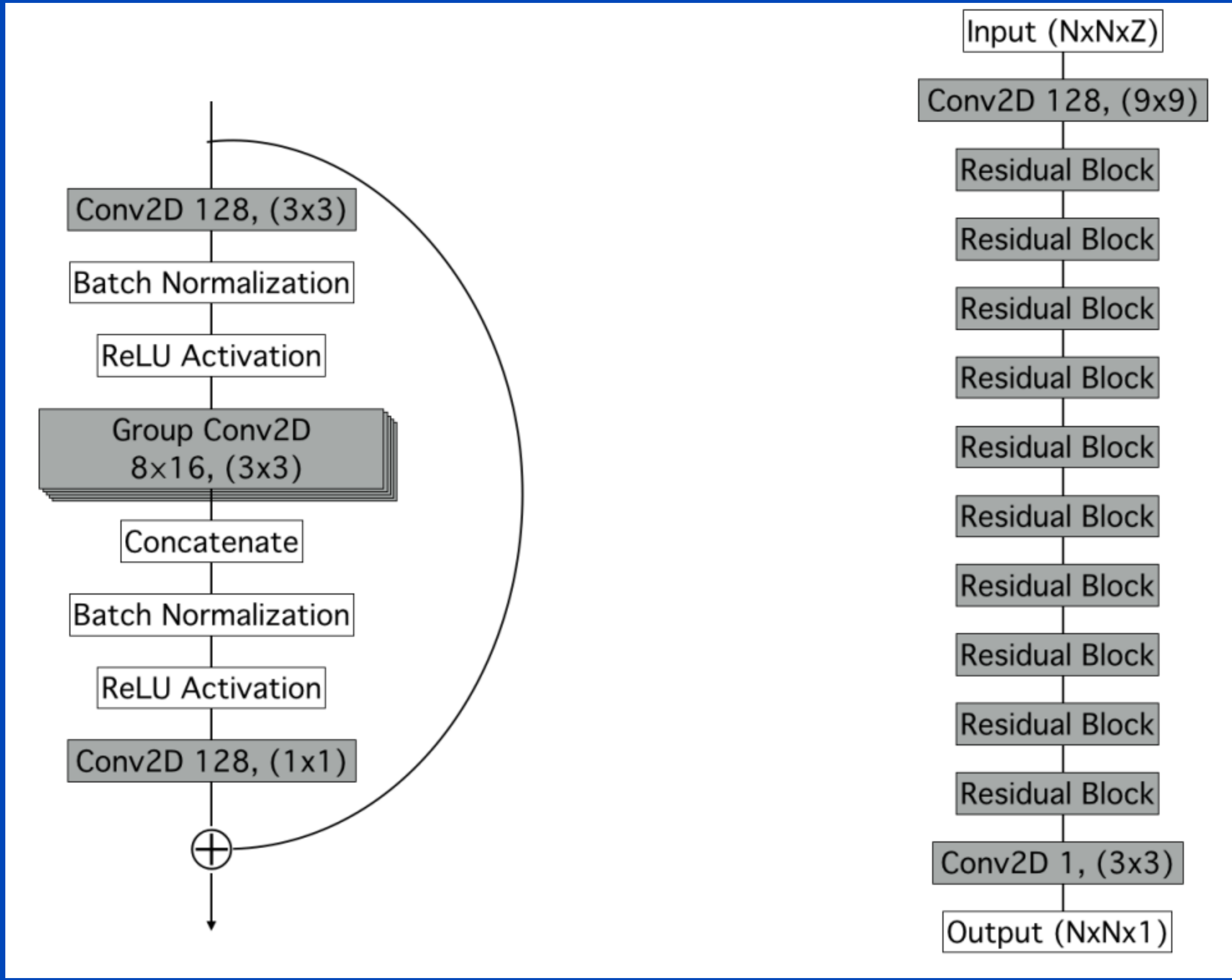

Image taken from [2]

- ResNet predicts the noise of the image
- The final prediction (a denoised image) is given by subtracting the output from the input

[2] A. D. Missert, S. Leng, L. Yu, and C. H. McCollough, “Noise subtraction for low-dose CT images using a deep convolutional neural network,” in Proceedings of the Fifth International Conference on Image Formation in X-Ray Computed Tomography, Salt Lake City, UT, USA, May 2018, pp. 399–402.

WGAN-VGG

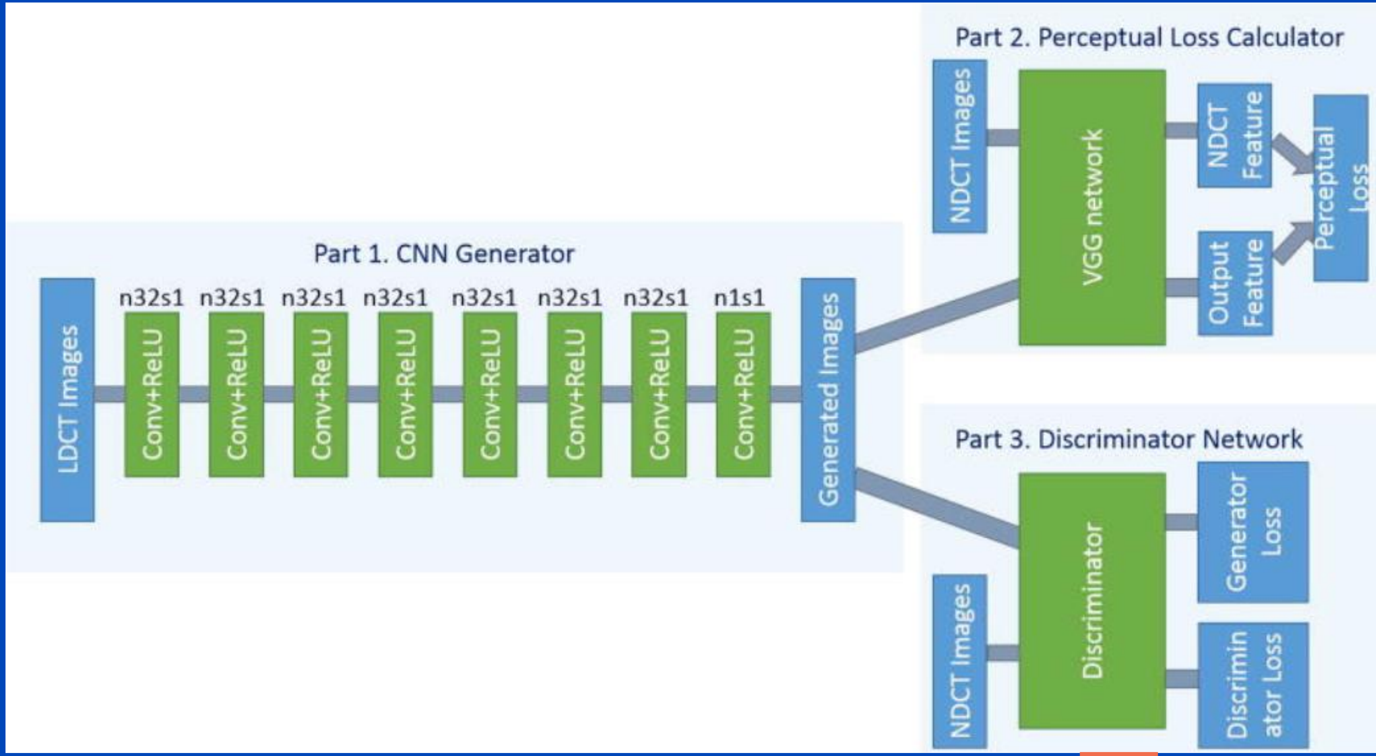

Images taken from [3]

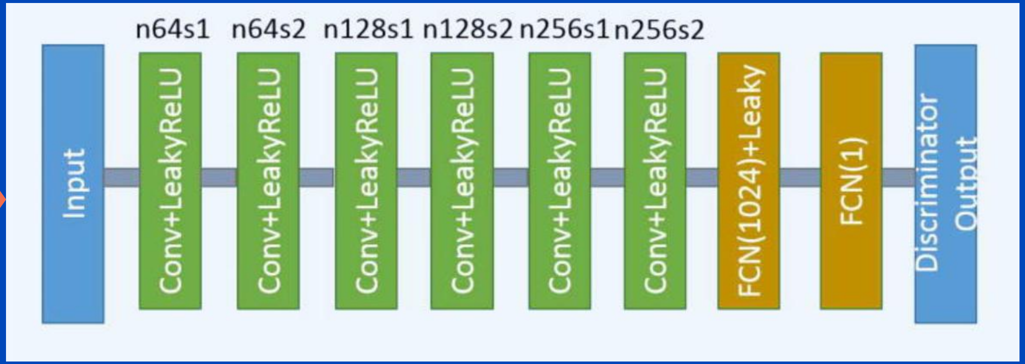

[3] Q. Yang, P. Yan, Y. Zhang, H. Yu, Y. Shi, X. Mou, M. K. Kalra, Y. Zhang, L. Sun, and G. Wang, "Low-dose CT image denoising using a generative adversarial network with wasserstein distance and perceptual loss," IEEE Transactions on Medical Imaging, vol. 37, no. 6, pp. 1348– 1357, June 2018.

Results

Std Dose | **10% Dose** | **WGAN**

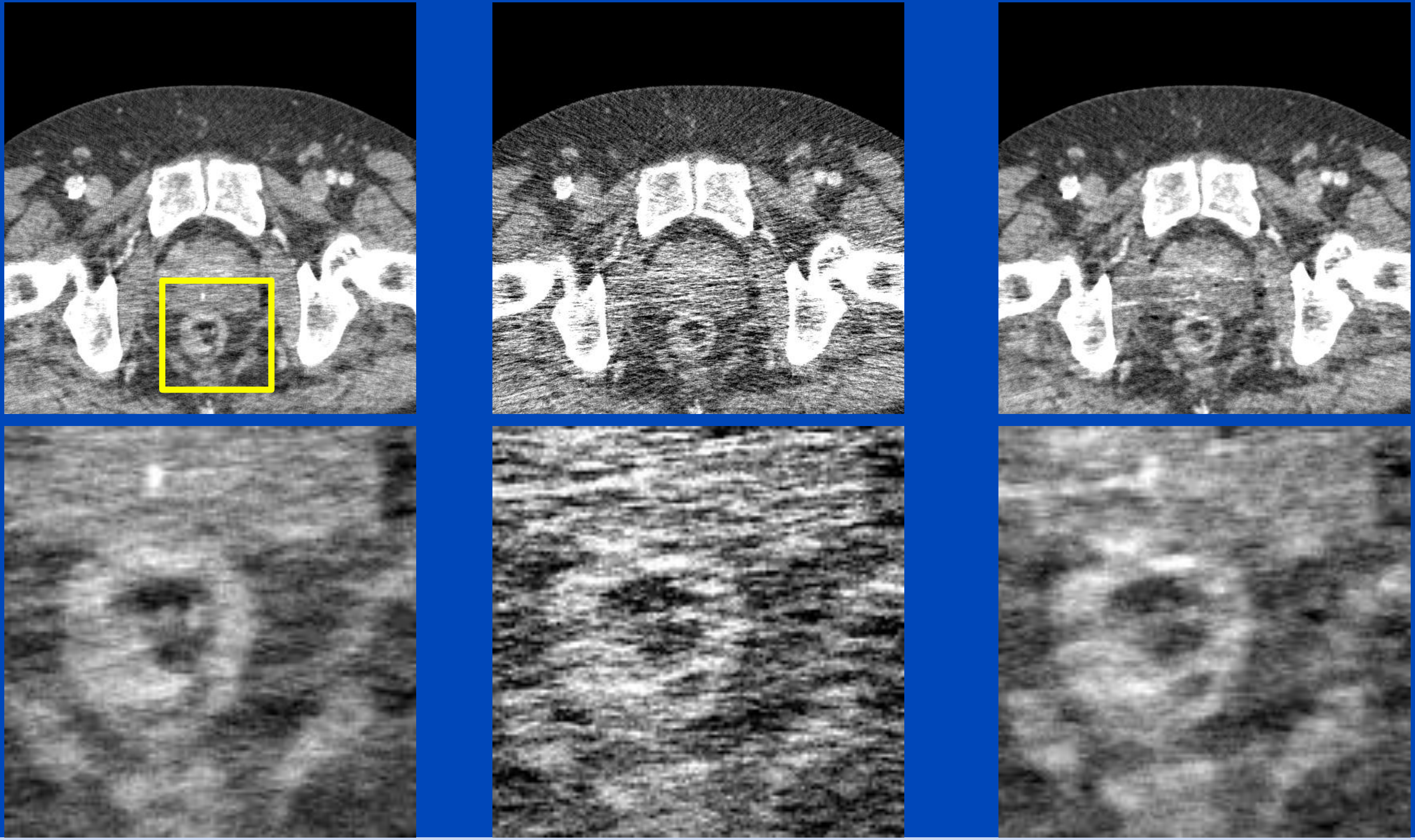

C = 0 HU, *W* = 500 HU

Results

Std Dose | **10% Dose** | **WGAN$_{+10}$**

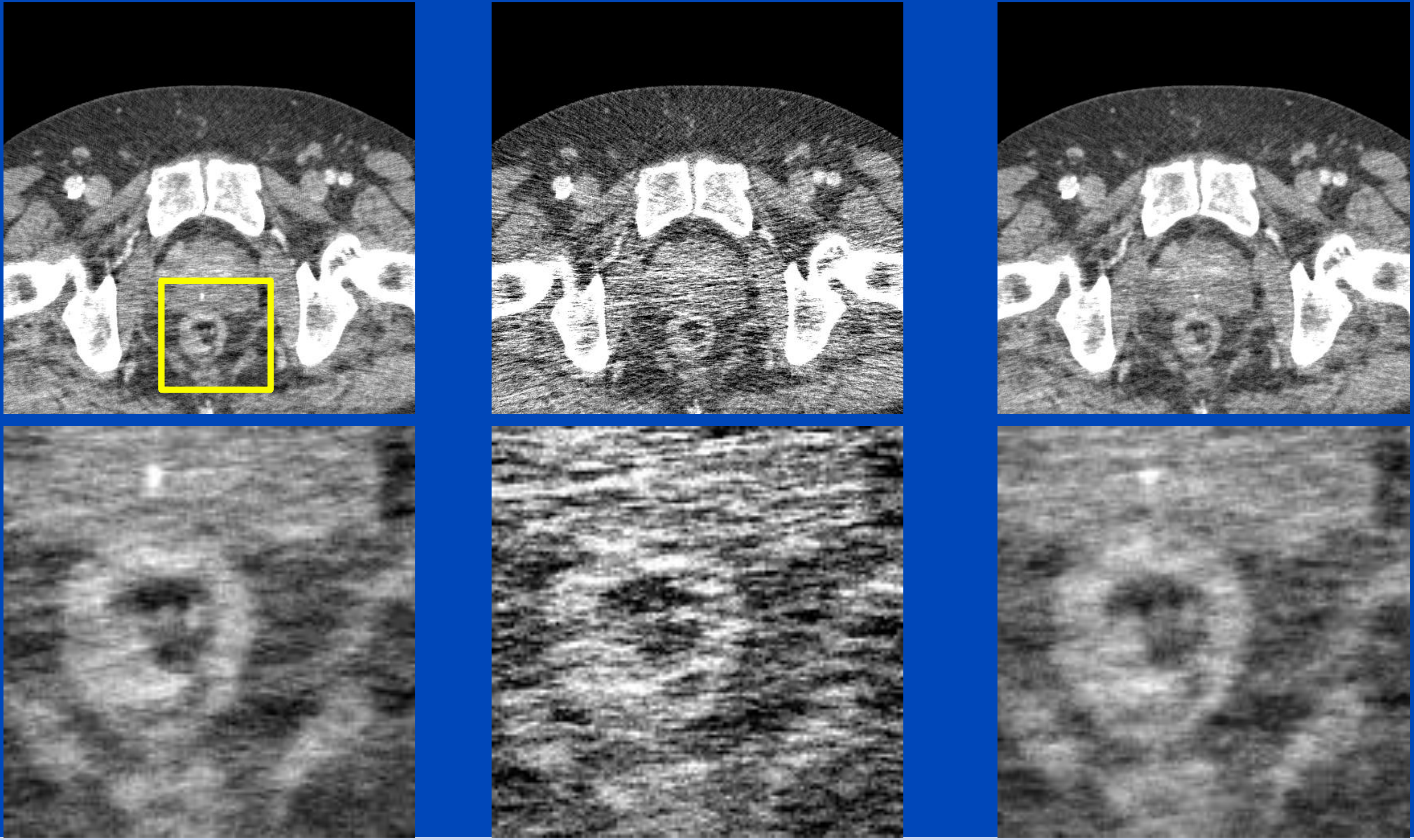

C = 0 HU, *W* = 500 HU

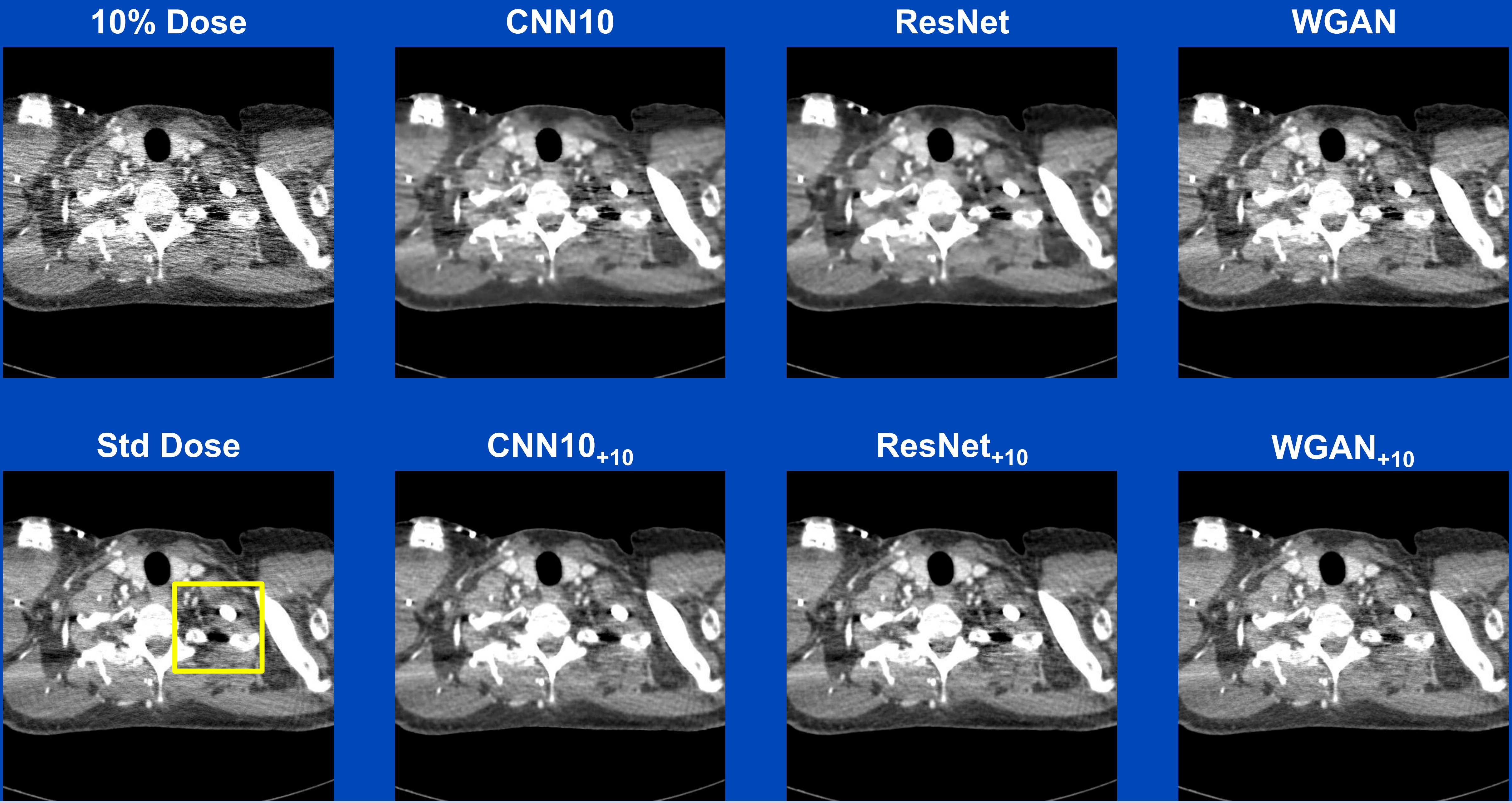

C = 0 HU, *W* = 600 HU

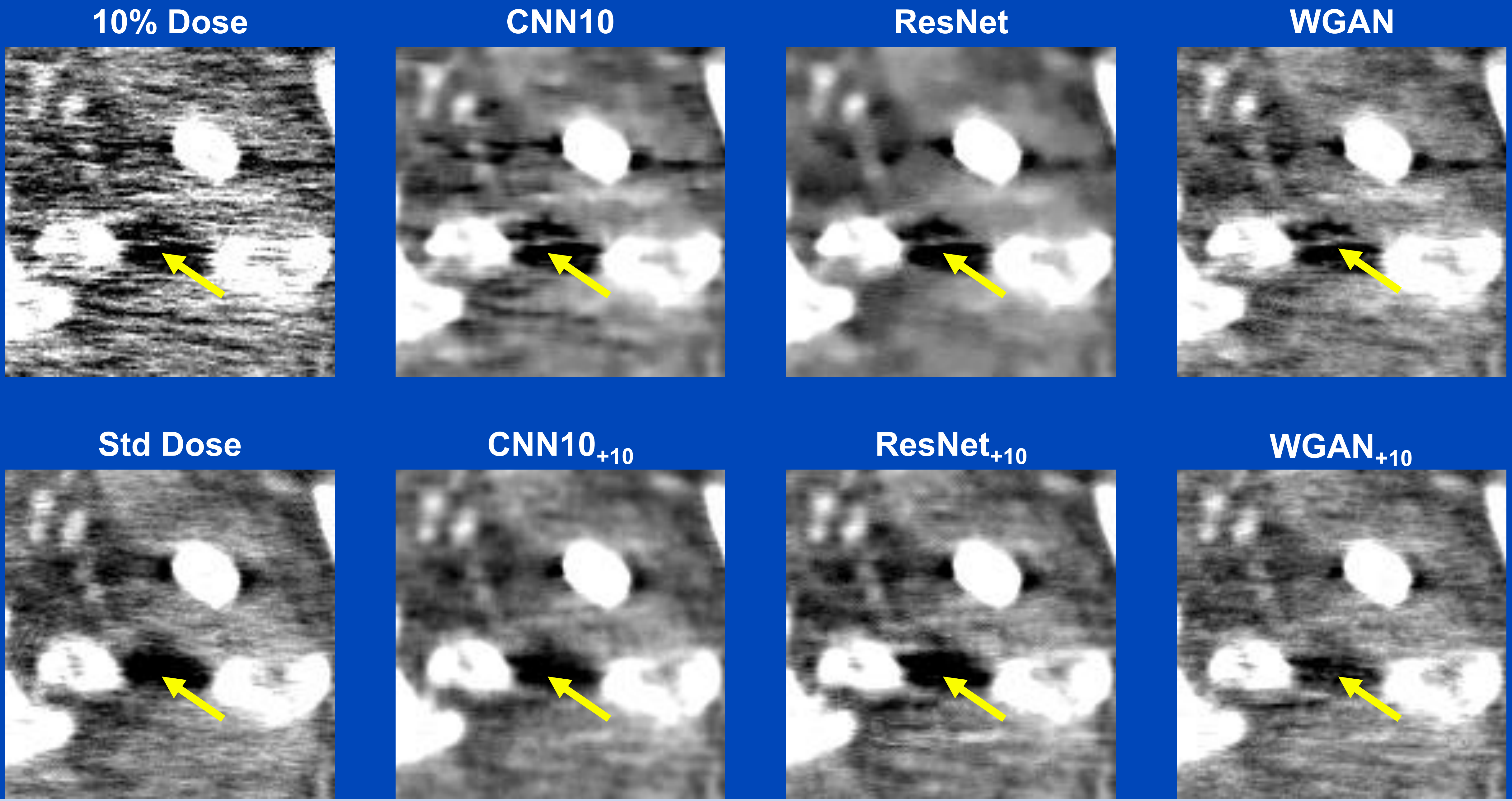

C = 0 HU, W = 600 HU

Siemens ReconCT

- **Proprietary software**
  - to reconstruct scanner rawdata
  - to inject noise into rawdata to simulate low dose scans
- **Allows to generate the 10 additional noise images needed for NADD.**

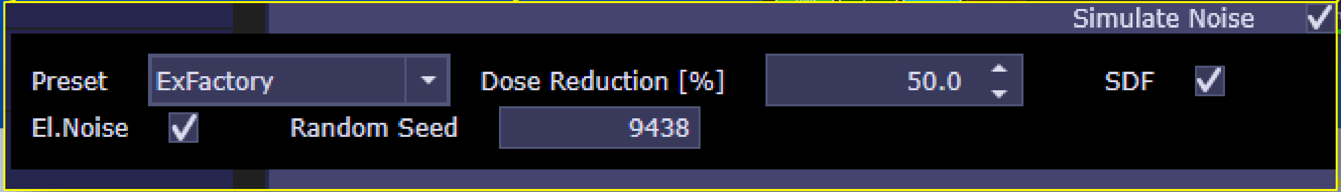

NADD Results

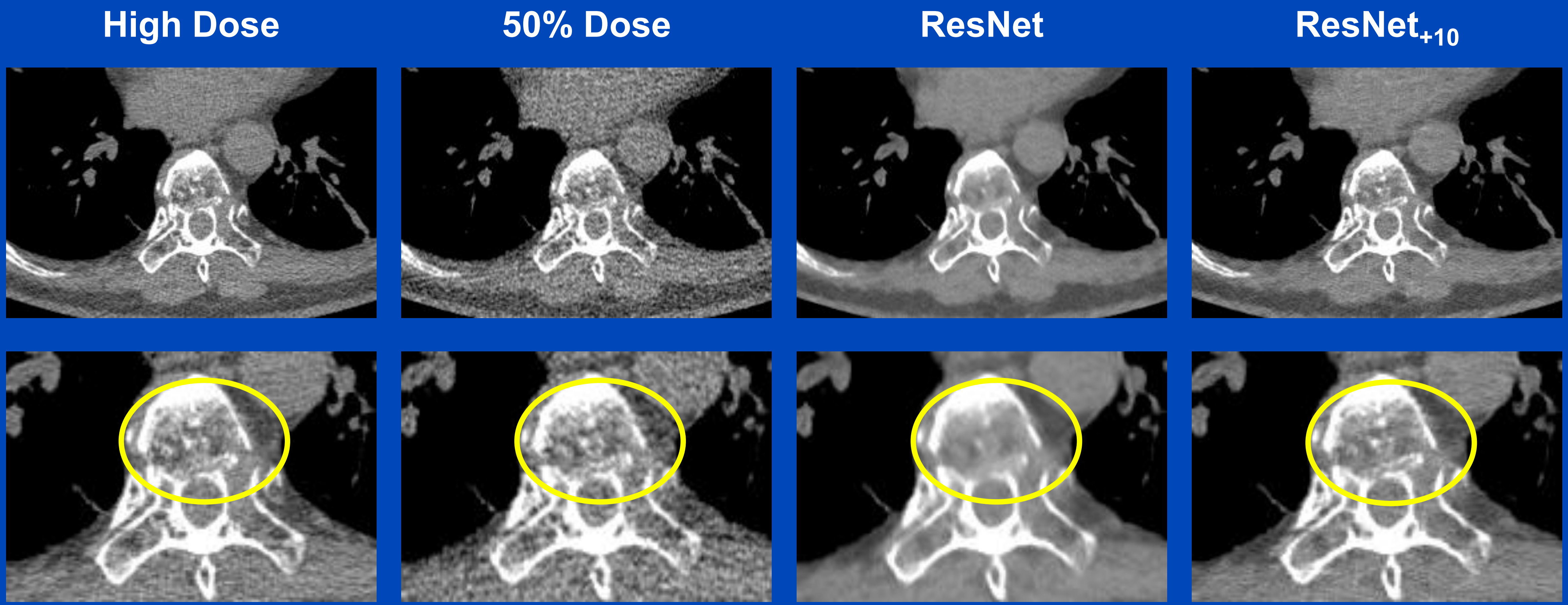

All images reconstructed with ReconCT using the B37f kernel. C = 30 HU, W = 660 HU

NADD Results

High Dose | 50% Dose | ResNet | ResNet$_{+10}$

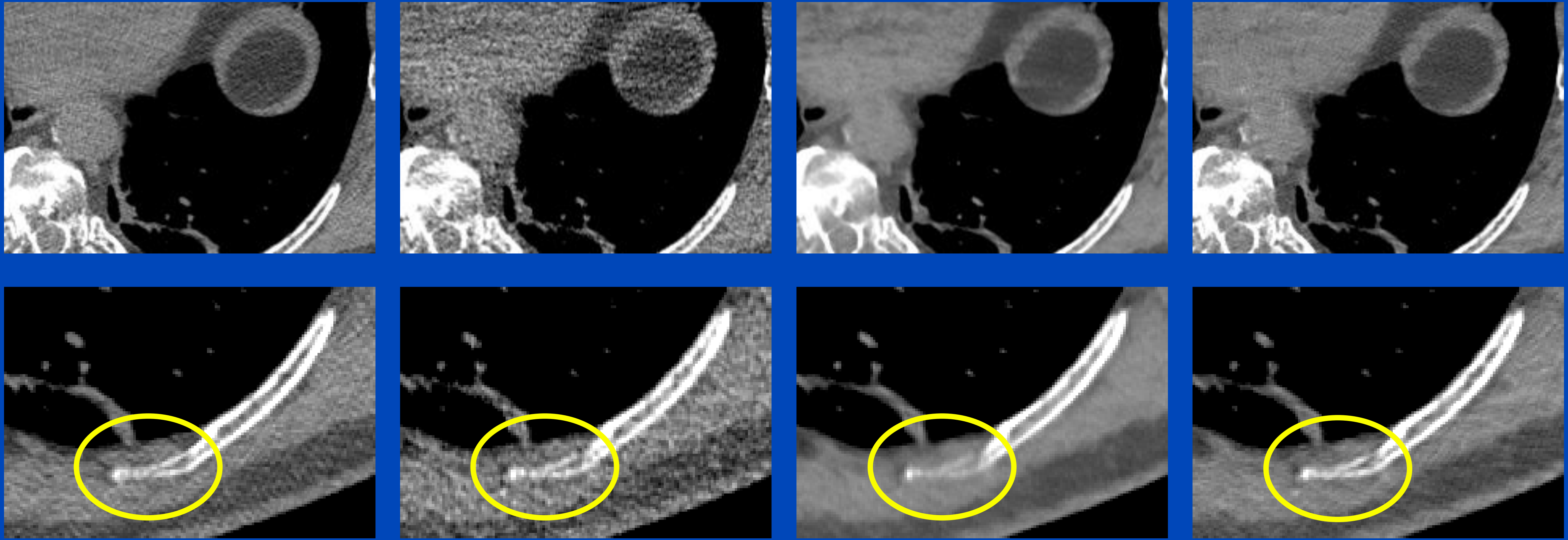

All images reconstructed with ReconCT using the B37f kernel. C = 30 HU, W = 660 HU

Deep Scatter Estimation

DSE

Monte Carlo Scatter Estimation

- Simulation of photon trajectories according to physical interaction probabilities.
- Simulating a large number of photon … approximates the actual scatter distrib…

1 to 10 hours
per tomographic data set

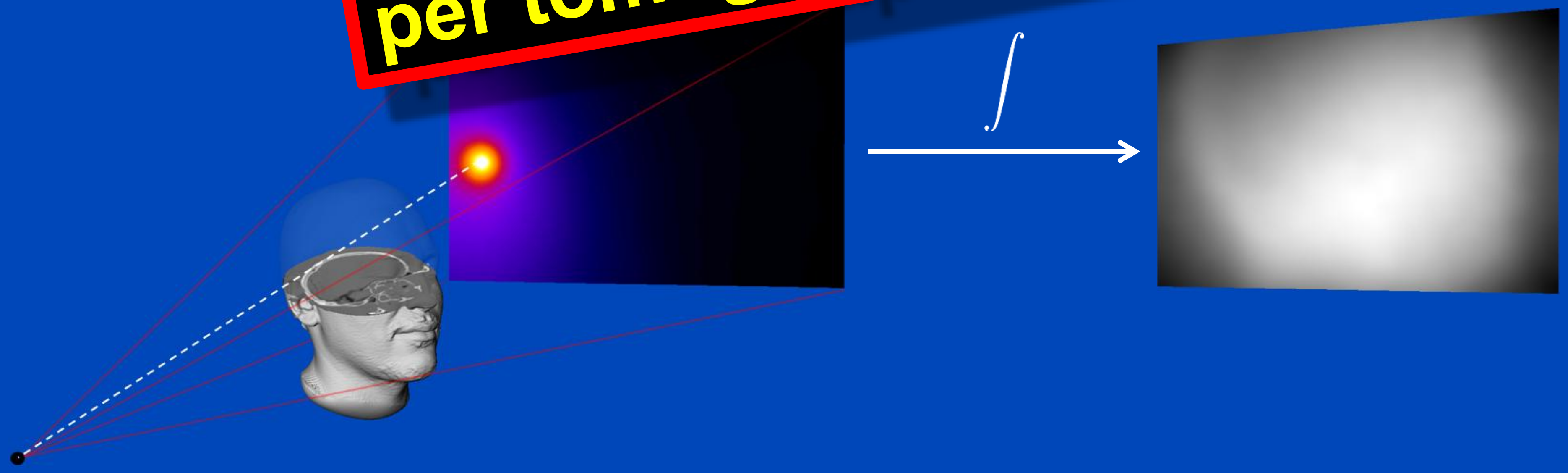

Deep Scatter Estimation

Network architecture & scatter estimation framework

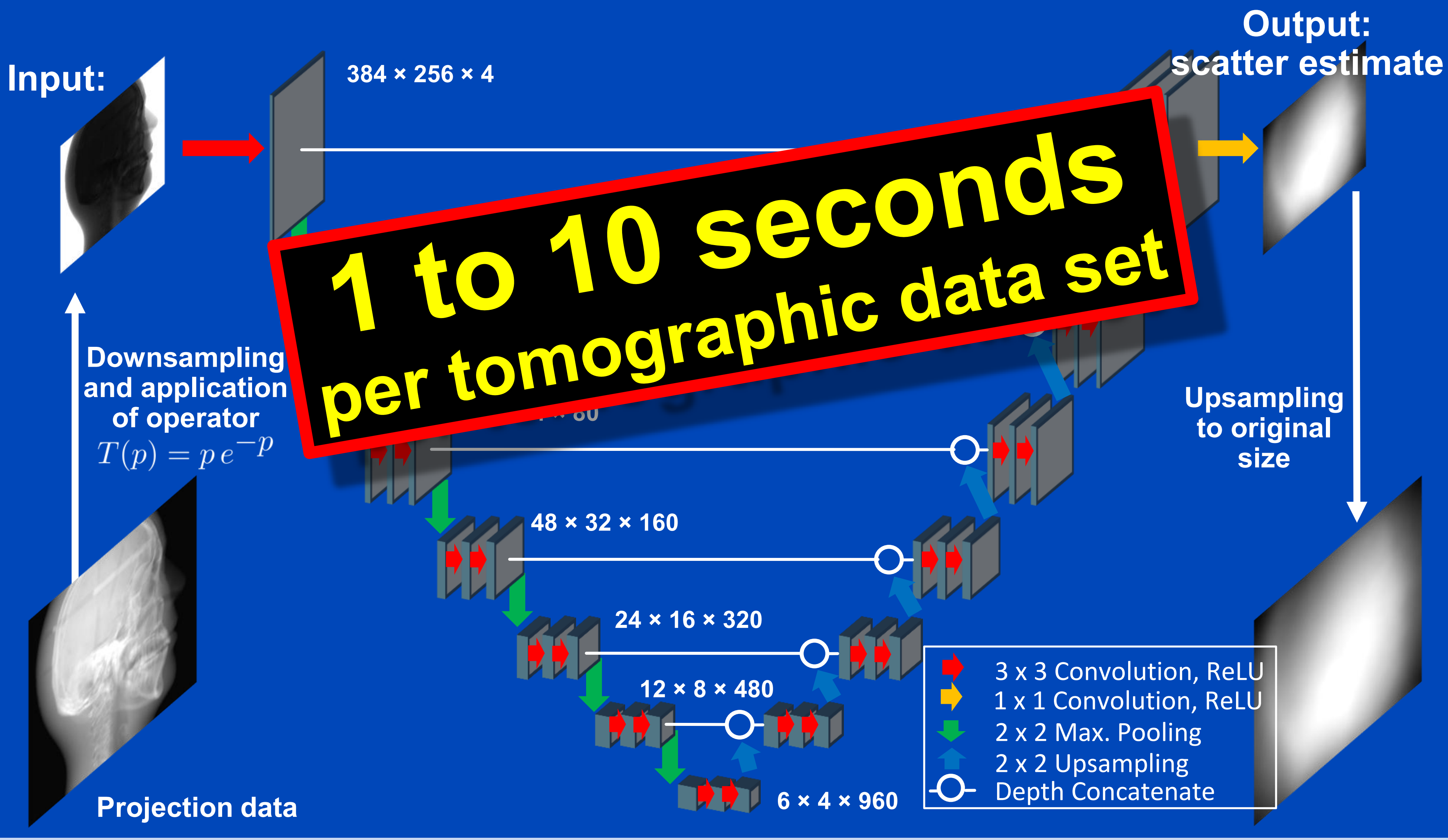

J. Maier, M. Kachelrieß et al. Deep scatter estimation (DSE). SPIE 2017 and Journal of Nondestructive Evaluation 37:57, July 2018.
J. Maier, M. Kachelrieß et al. Robustness of DSE. Med. Phys. 46(1):238-249, January 2019.

Ref 1: Kernel-Based Scatter Estimation

- **Kernel-based scatter estimation[1]:**
  - **Estimation of scatter by a convolution of the scatter source term *T*(*p*) with a scatter propagation kernel *G*(*u*, *c*):**

$$I_{\mathrm{s,\ est}}(\boldsymbol{u}) = \underbrace{\left(c_0 \cdot p(\boldsymbol{u}) \cdot e^{-p(\boldsymbol{u})}\right)}_{T(p)(\boldsymbol{u})} * \underbrace{\left(\sum_{\pm} e^{-c_1(\boldsymbol{u}\hat{\boldsymbol{e}}_1 \pm c_2)^2} \cdot \sum_{\pm} e^{-c_3(\boldsymbol{u}\hat{\boldsymbol{e}}_2 \pm c_4)^2}\right)}_{G(\boldsymbol{u},\boldsymbol{c})}$$

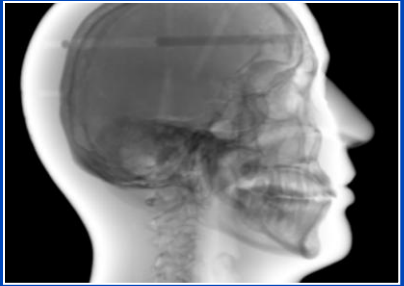

$T(p)(\boldsymbol{u})$

Open parameters:

c_0

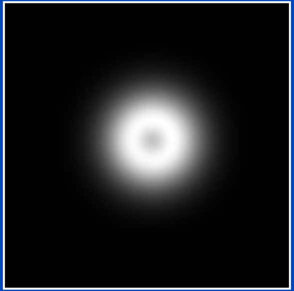

$G(\boldsymbol{u}, \boldsymbol{c})$

Open parameters:

c_1, c_2, c_3, c_4

$$\{c_i\} = \operatorname{argmin} \sum_n \sum_{\boldsymbol{u}} \left\| I_{\mathrm{s,\ est}}(n, \boldsymbol{u}, \{c_i\}) - I_{\mathrm{s}}(n, \boldsymbol{u}) \right\|_2^2,$$

Samples of the training data set

Detector coordinate

Scatter estimate

MC scatter simulation

[1] B. Ohnesorge, T. Flohr, K. Klingenbeck-Regn: Efficient object scatter correction algorithm for third and fourth generation CT scanners. Eur. Radiol. 9, 563–569 (1999).

Ref 2: Hybrid Scatter Estimation

- **Hybrid scatter estimation[2] :**
  - Estimation of scatter by a convolution of the scatter source term *T*(*p*) with a scatter propagation kernel *G*(*u*, *c*):

$$I_{\mathrm{s,\ est}}(\boldsymbol{u}) = \underbrace{\left(c_0 \cdot p(\boldsymbol{u}) \cdot e^{-p(\boldsymbol{u})}\right)}_{T(p)(\boldsymbol{u})} * \underbrace{\left(\sum_{\pm} e^{-c_1(\boldsymbol{u}\hat{\boldsymbol{e}}_1 \pm c_2)^2} \cdot \sum_{\pm} e^{-c_3(\boldsymbol{u}\hat{\boldsymbol{e}}_2 \pm c_4)^2}\right)}_{G(\boldsymbol{u},\boldsymbol{c})}$$

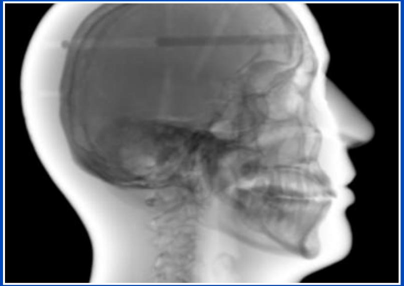

$T(p)(\boldsymbol{u})$

Open parameters: c_0

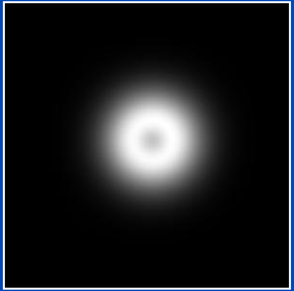

$G(\boldsymbol{u}, \boldsymbol{c})$

Open parameters: c_1, c_2, c_3, c_4

$$\underbrace{\{c_i\}_n}_{\text{Samples of the test data set}} = \operatorname{argmin} \sum_{\underbrace{\boldsymbol{u}}_{\text{Detector coordinate}}} \|\underbrace{I_{\mathrm{s,\ est}}(n, \boldsymbol{u}, \{c_i\})}_{\text{Scatter estimate}} - \underbrace{I_{\mathrm{s}}(n, \boldsymbol{u})}_{\text{Coarse MC simulation}}\|_2^2,$$

Scatter estimate

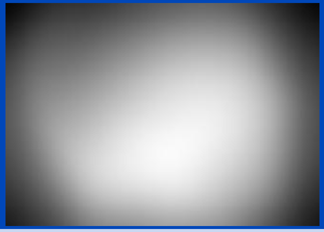

Coarse MC simulation

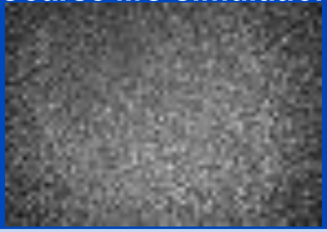

[2] M. Baer, M. Kachelrieß: Hybrid scatter correction for CT imaging. Phys. Med. Biol. 57, 6849–6867 (2012).

dkfz.

Reconstructions of Simulated Data

Parameters of the two comparison methods trained in the same way as those of DSE: same data, same loss function, same optimization algorithm.

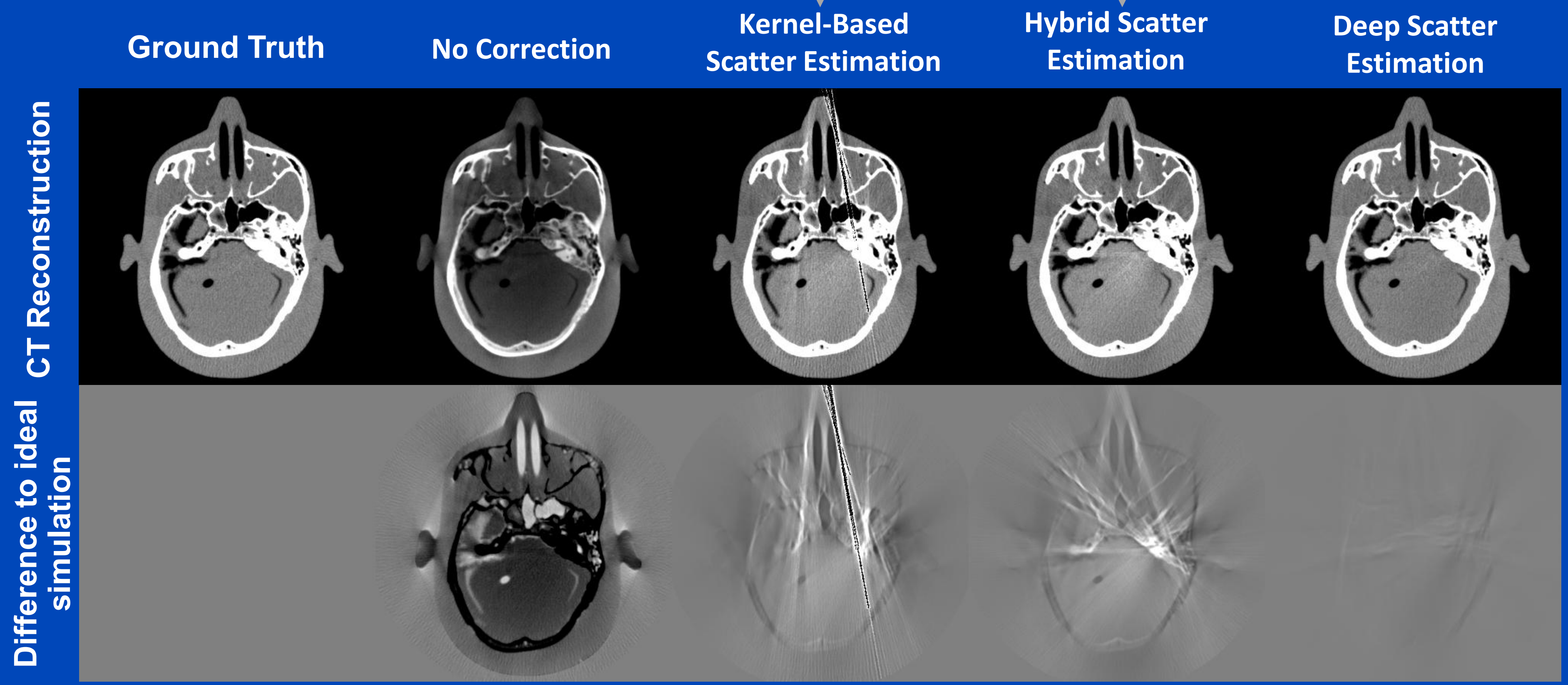

C = 0 HU, W = 1000 HU

J. Maier, M. Kachelrieß et al. Deep scatter estimation (DSE). SPIE 2017 and Journal of Nondestructive Evaluation 37:57, July 2018.
J. Maier, M. Kachelrieß et al. Robustness of DSE. Med. Phys. 46(1):238-249, January 2019.

Testing of the DSE Network for Measured Data (120 kV)

DKFZ table-top CT

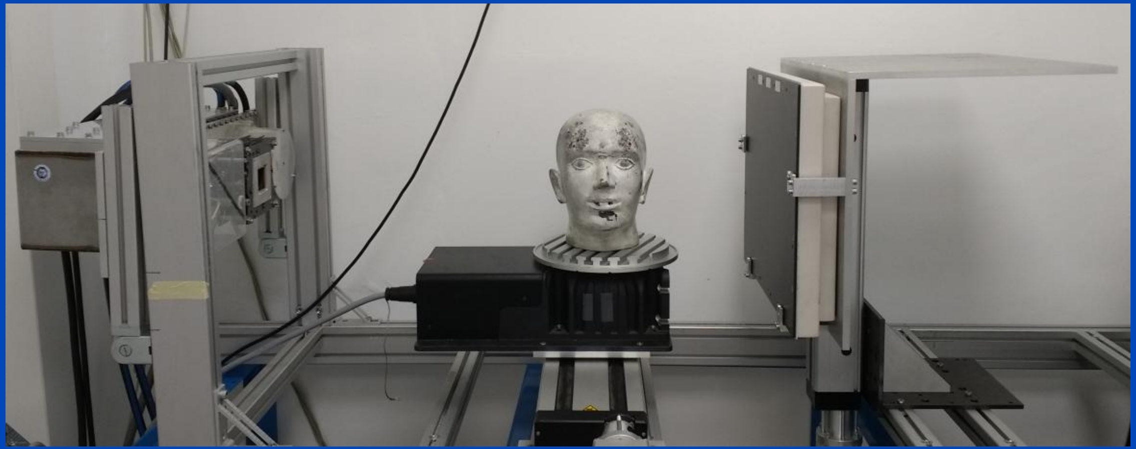

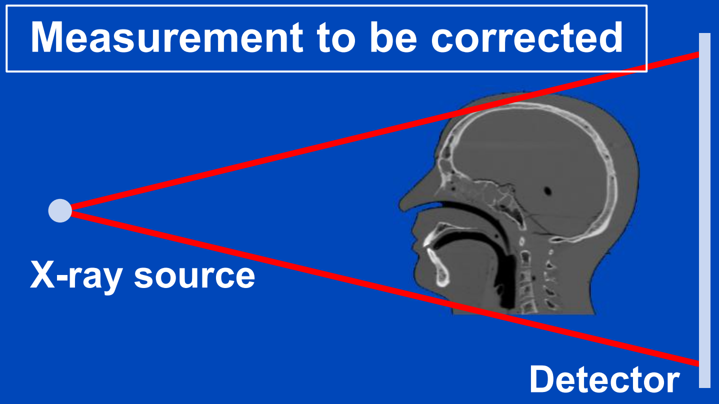

- Measurement of a head phantom at our in-house table-top CT.
- Slit scan measurement serves as ground truth.

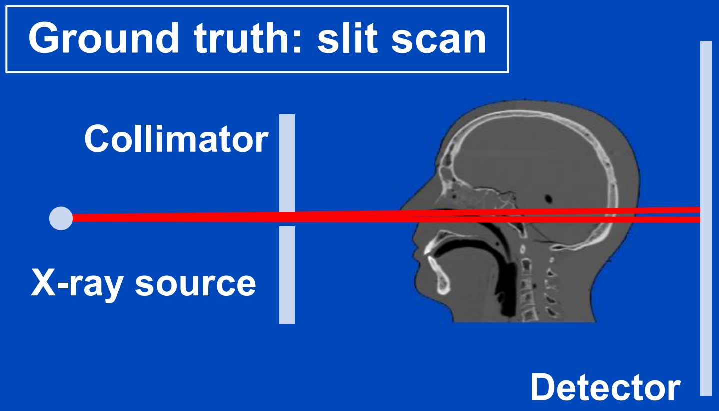

J. Maier, M. Kachelrieß et al. Deep scatter estimation (DSE). SPIE 2017 and Journal of Nondestructive Evaluation 37:57, July 2018.
J. Maier, M. Kachelrieß et al. Robustness of DSE. Med. Phys. 46(1):238-249, January 2019.

dkfz.

Reconstructions of Measured Data

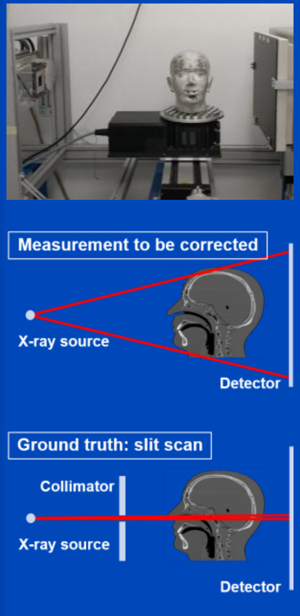

Parameters of the two comparison methods trained in the same way as those of DSE: same data, same loss function, same optimization algorithm.

Slit Scan	No Correction	Kernel-Based Scatter Estimation	Hybrid Scatter Estimation	DSE Deep Scatter Estimation

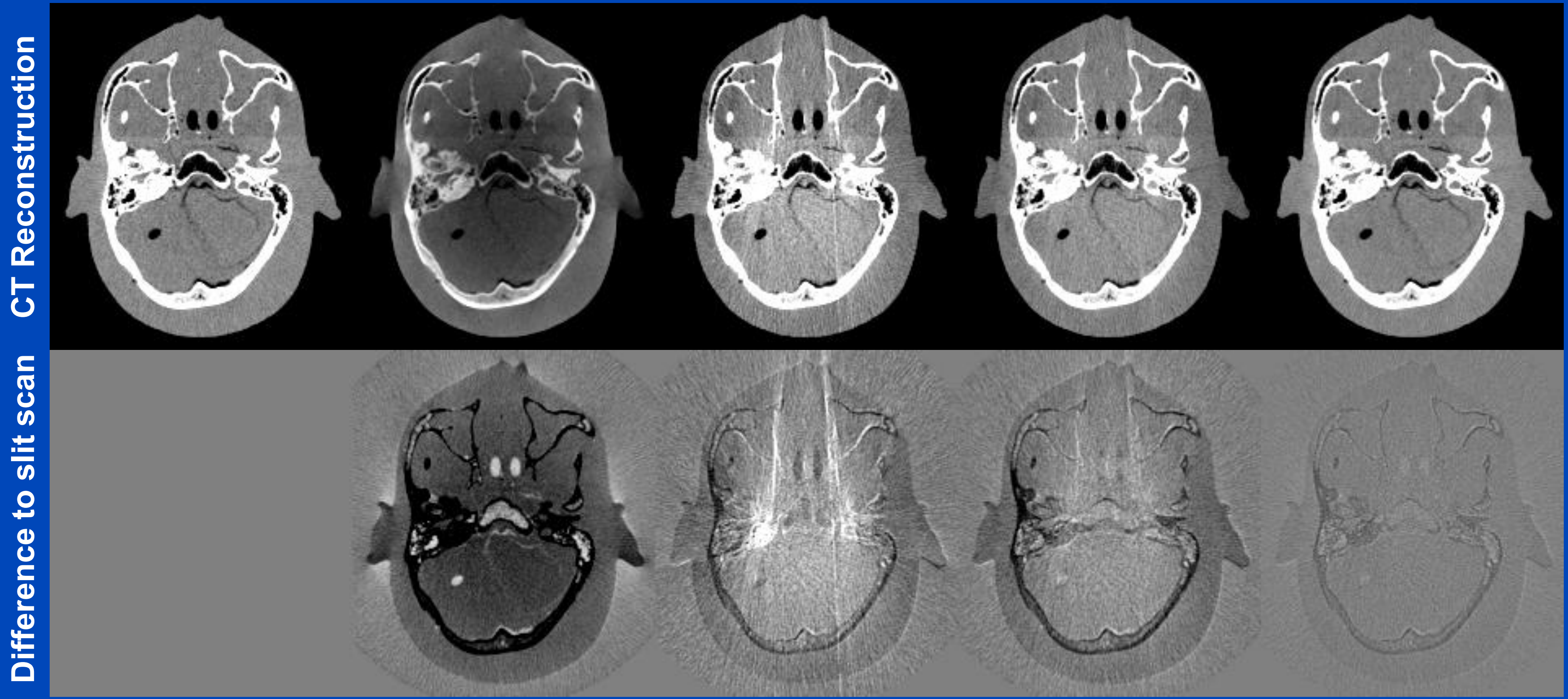

C = 0 HU, W = 1000 HU

J. Maier, M. Kachelrieß et al. Deep scatter estimation (DSE). SPIE 2017 and Journal of Nondestructive Evaluation 37:57, July 2018.
J. Maier, M. Kachelrieß et al. Robustness of DSE. Med. Phys. 46(1):238-249, January 2019.

A simple detruncation was applied to the rawdata before reconstruction. Images were clipped to the FOM before display. C = -200 HU, W = 1000 HU.

Truncated DSE

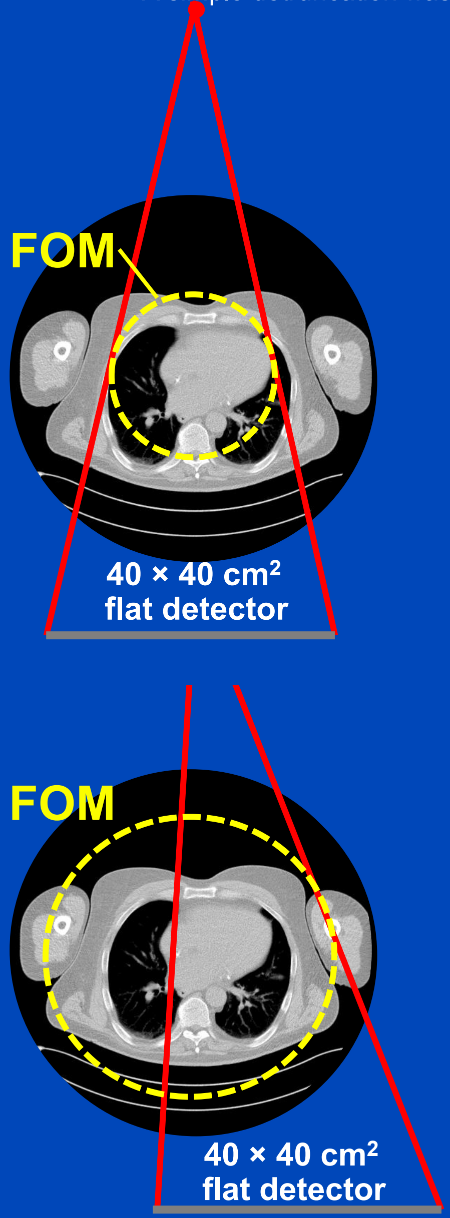

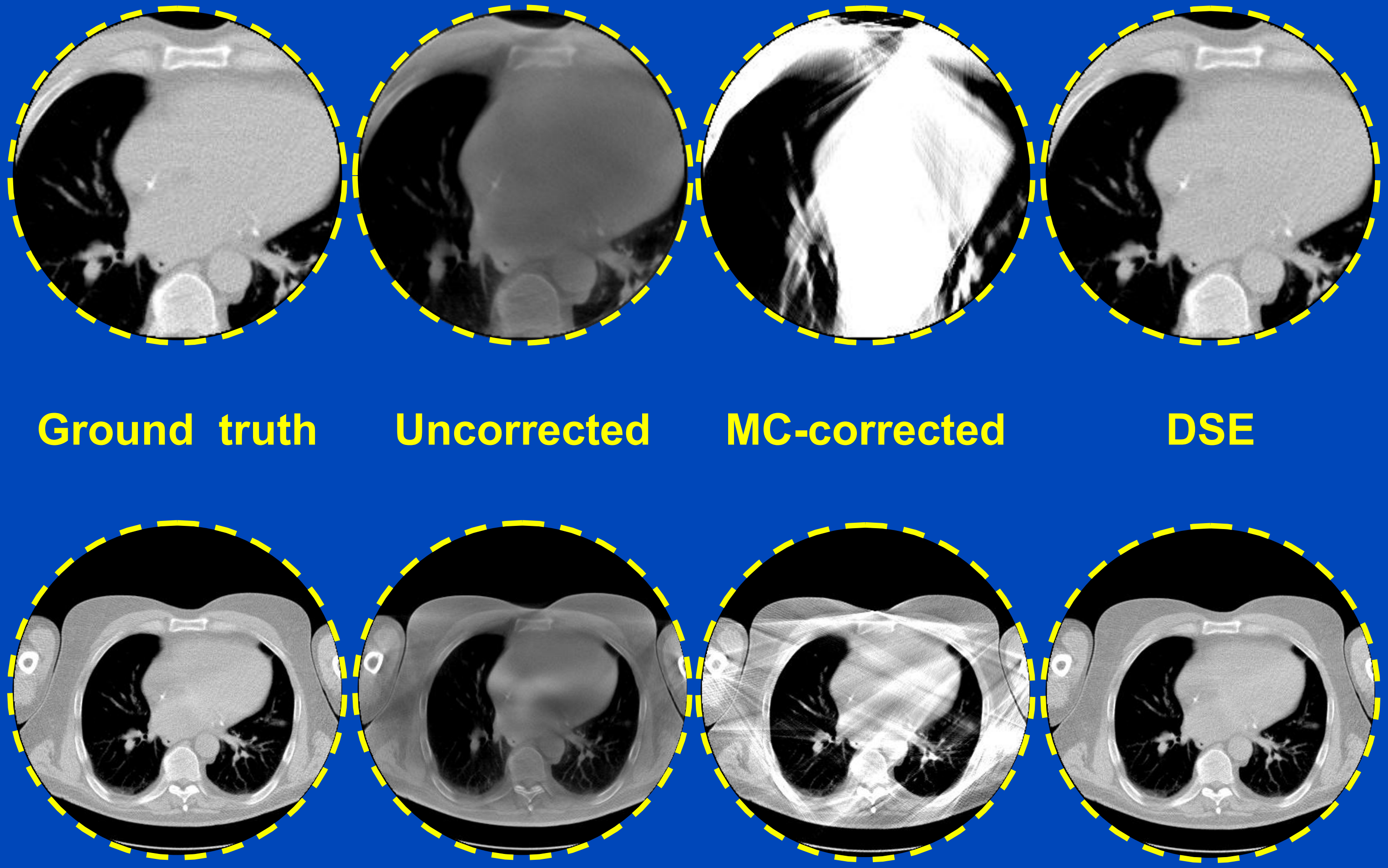

To learn why MC fails at truncated data and what significant efforts are necessary to cope with that situation see [Kachelrieß et al. Effect of detruncation on the accuracy of MC-based scatter estimation in truncated CBCT. Med. Phys. 45(8):3574-3590, August 2018].

J. Maier, M. Kachelrieß et al. Deep scatter estimation (DSE). SPIE 2017 and Journal of Nondestructive Evaluation 37:57, July 2018.
J. Maier, M. Kachelrieß et al. Robustness of DSE. Med. Phys. 46(1):238-249, January 2019.

Does DSE Generalize to Different Anatomical Regions?

- **DSE:**

DSE	Head	Thorax	Abdomen
Head	1.2	21.1	32.7
Thorax	8.8	1.5	9.1
Abdomen	11.9	10.9	1.3
All data	1.8	1.4	1.4

Values shown are the mean absolute percentage errors (MAPEs) of the testing data.
Note that thorax and head suffer from truncation due to the small size of the 40×30 cm flat detector.

- **KSE** (“trained” using the same data):

KSE	Head	Thorax	Abdomen
Head	14.5	26.8	32.5
Thorax	16.2	18.5	19.4
Abdomen	16.8	22.1	17.8
All data	14.9	20.5	19.3

J. Maier, M. Kachelrieß et al. Deep scatter estimation (DSE). SPIE 2017 and Journal of Nondestructive Evaluation 37:57, July 2018.
J. Maier, M. Kachelrieß et al. Robustness of DSE. Med. Phys. 46(1):238-249, January 2019.

Measurement-Based Data Generation

- Naeotom Alpha (Siemens Healthineers AG, Forchheim, Germany)
- Several phantoms (water phantoms, multi-energy QA phantoms, and anthropomorphic phantoms) are used in the data set.
- Fully automated measurement script
- Patient table z-position in steps of 5 cm
- Random table height (±8 cm around the isocenter)
- Two scans at each table position
  - 6 × 0.4 mm = 2.4 mm
  - 144 × 0.4 mm = 57.6 mm
- Default bowtie filter
- Energy thresholds T_1 = 20 keV, T_2 = 65 keV
- 0.5 s circle scans with 140 kV and 100 mAs / rotation

Total training data set: 5760 projections
36 projections per z-position
160 different z-positions

Measurement-Based DSE (mbDSE)

- **Perform two scans:**
  - Scan with full collimation. It contains scatter and primary intensity.
  - Scan with narrow collimation (slit scan). It contains primary only, scatter is negligible.
- **Scatter intensity:**
  - The difference between the intensities of full and narrow collimated data is used as label.
  - Only the data within the primary fan of the narrow collimated scan are used.

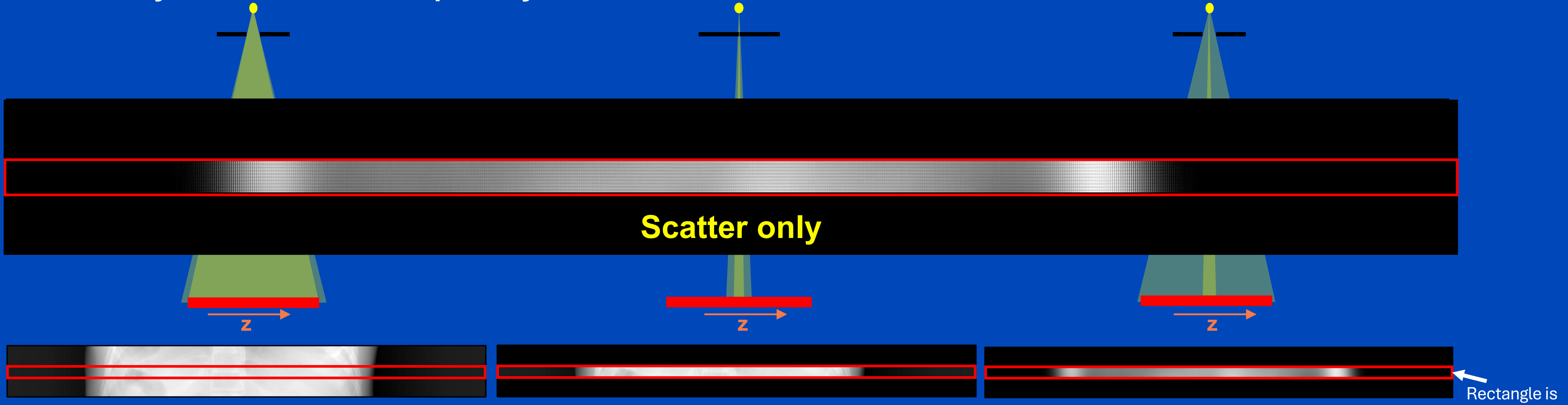

Full collimation (144 × 0.4 mm):
Primary + scatter

Narrow collimation (6 × 0.4 mm):
Primary only

Difference:
Scatter only

Deep Physics Prior Normalized Metal Artifact Reduction

dppNMAR

Normalized MAR (NMAR)

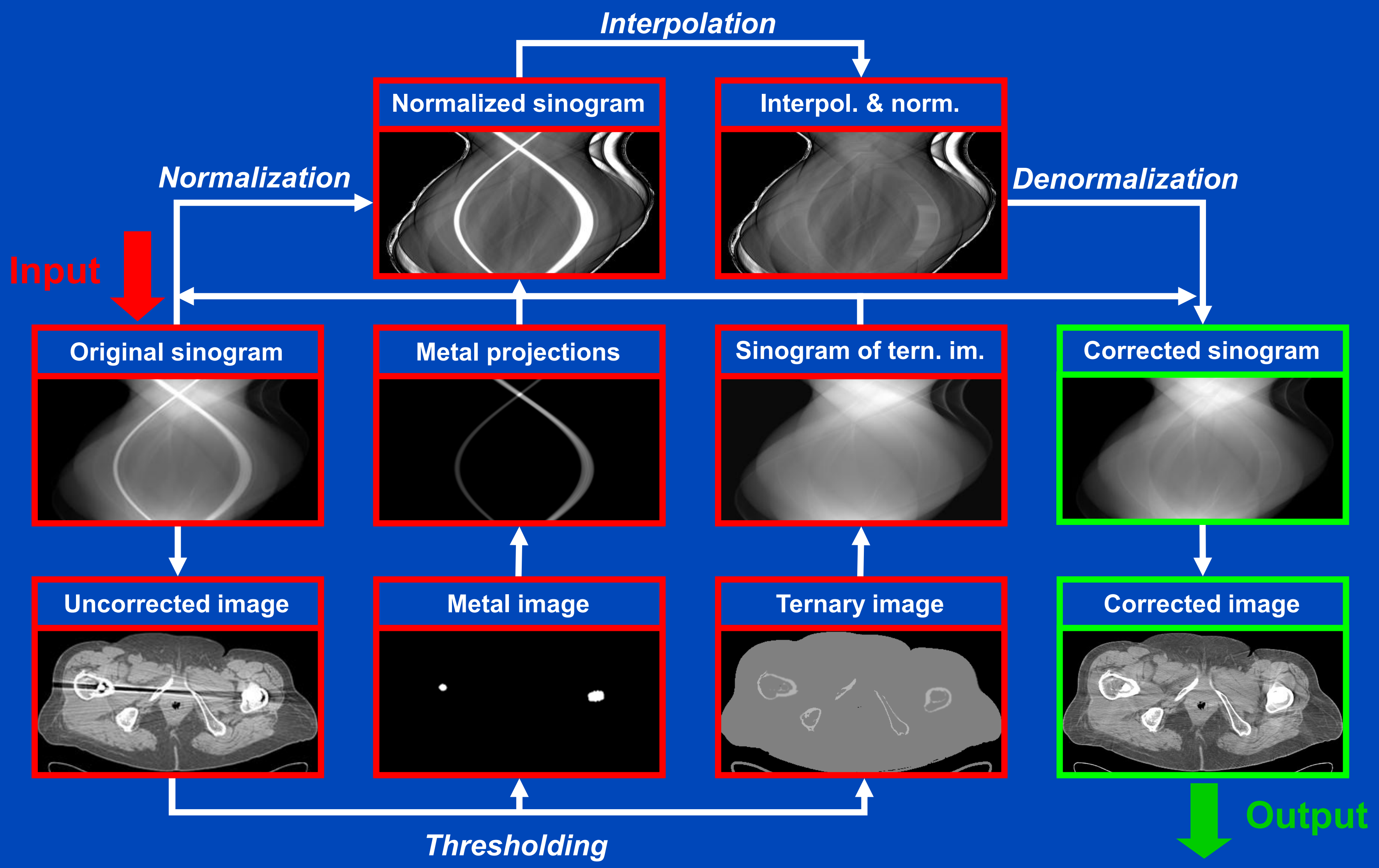

E. Meyer, R. Raupach, M. Lell, B. Schmidt, and M. Kachelrieß, “Normalized metal artifact reduction (NMAR) in CT”, Med. Phys. 37(10):5482-5493, 2010.

Additional Spatial Information

Empirical Beam Hardening Correction (EBHC)

- **EBHC[1] and sfEBHC[2] idea: empirical beam-hardening correction using material-basis images and linear combination.**
- **Material basis images: energy-dependent functions.**

$$\mu(E,\boldsymbol{r}) = f_0(\boldsymbol{r})\psi_0(E) + f_2(\boldsymbol{r})\psi_2(E)$$

- **Projections: Compute sinograms p_0 and p_2 from images f_0, and f_2.**
- **Series expansion up to second order:**

$$\hat{p}_1 \approx \underbrace{p_0 + c_{01}p_2}\; + \;\underbrace{c_{11}p_0p_2}\; + \;\underbrace{c_{02}p_2^2}\; + \cdots$$

- **Reconstruction:** $f_{11} = \mathsf{X}^{-1}p_0p_2$

  $f_{02} = \mathsf{X}^{-1}p_2^2$

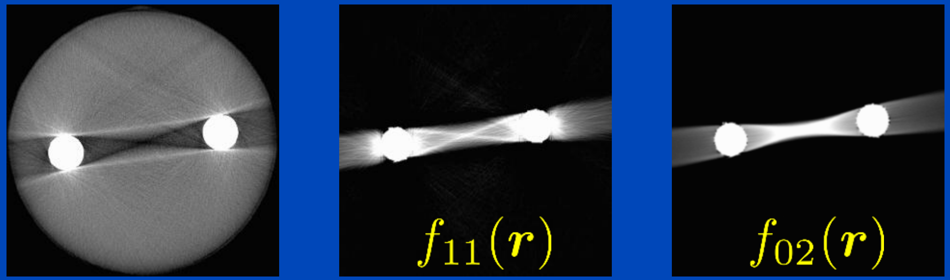

[1]Y. Kyriakou, E. Meyer, D. Prell, and M. Kachelrieß, "Empirical beam hardening correction (EBHC) for CT", Med. Phys. 37(10):5179-5187, October 2010.

[2]S. Schüller, S. Sawall, and M. Kachelrieß, "Segmentation-free empirical beam hardening correction for CT", Med. Phys. 42(2):794-803, February 2015.

Proposed Method

Deep Physics Prior Normalized Metal Artifact Reduction (dppNMAR)

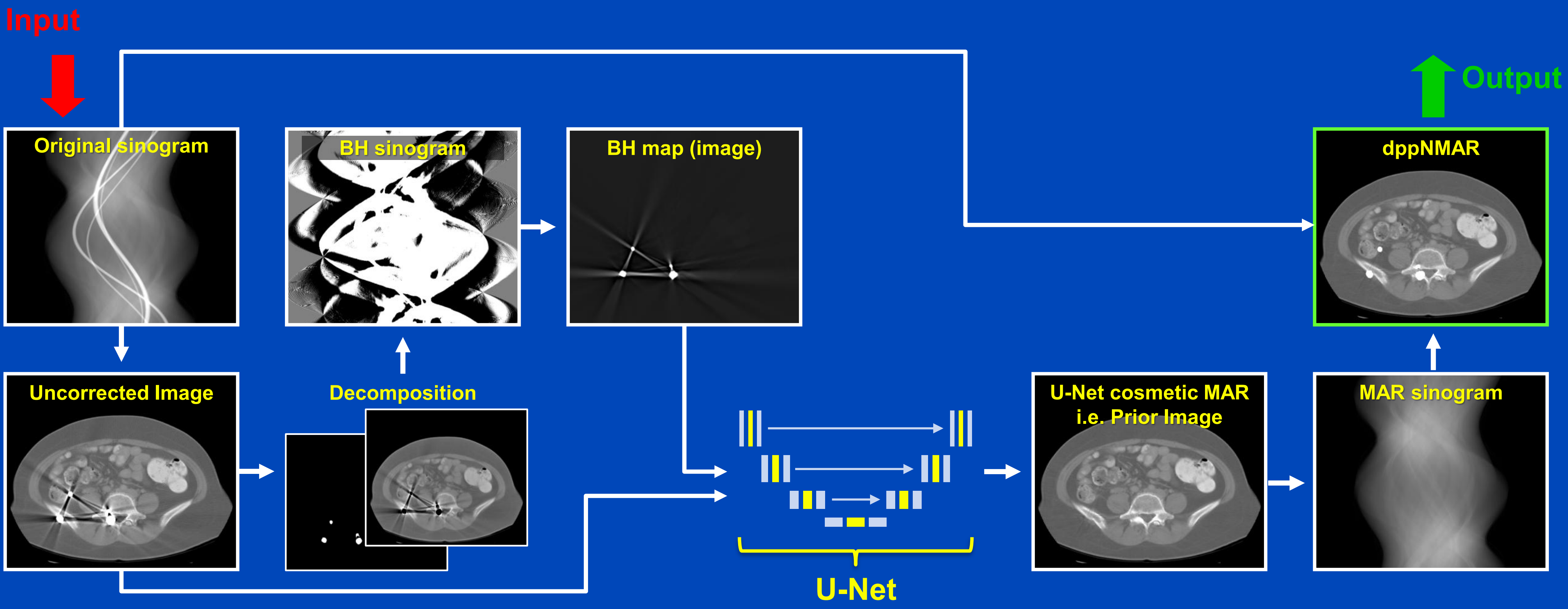

Network output is not seen by the reader!

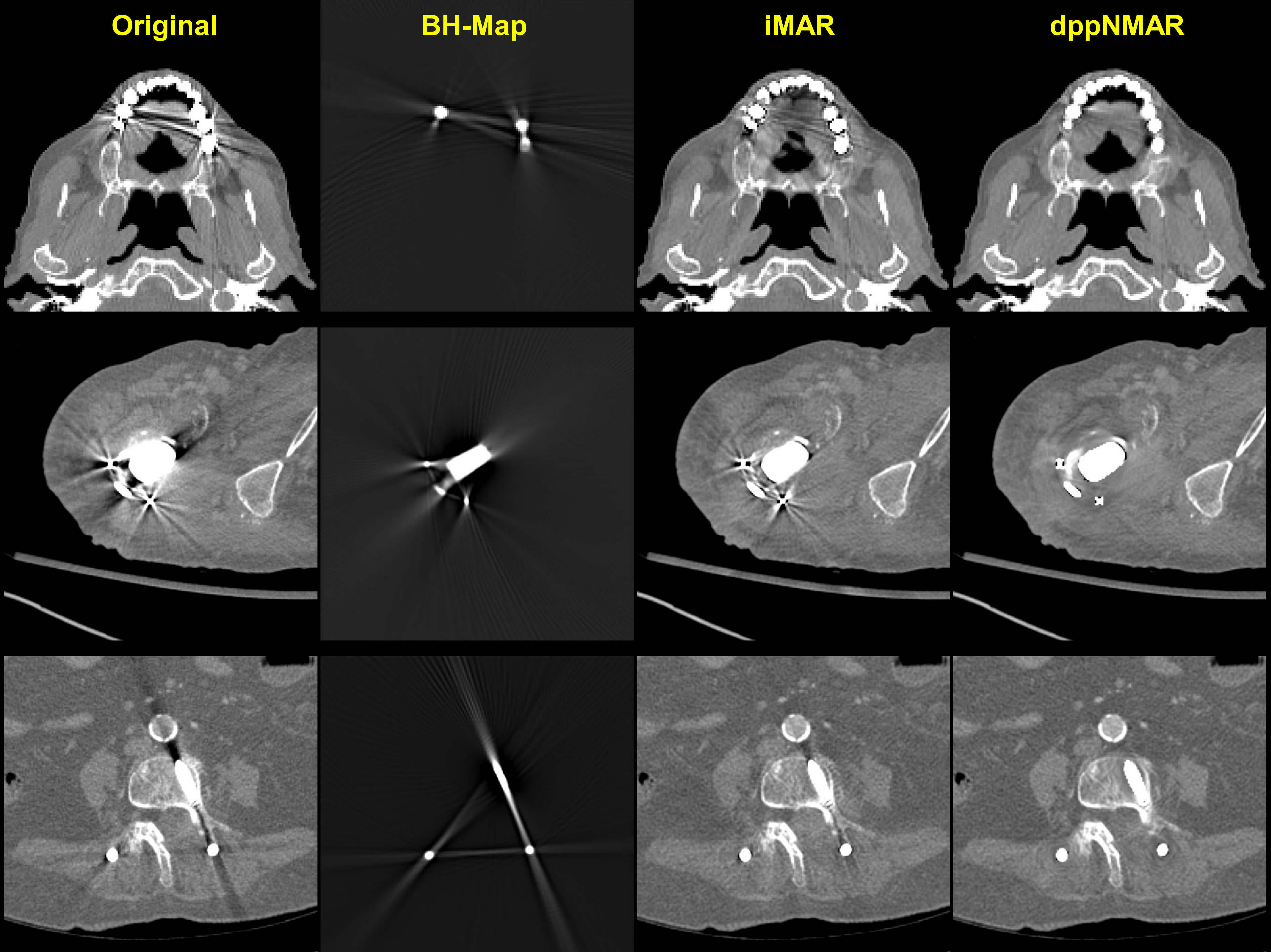

Siemens
Naeotom Alpha
140 kV
Qr48f
S_{eff} = 1.0 mm
C = 50 HU
W = 1200 HU

SIEMENS Healthineers

dkfz.

Deep Single Angle Motion Compensation

DEEP SAMOCO = TRUE 4D

Deep Cosmetic Motion Artifact Reduction

- Image-based correction
  = cosmetic correction
  = similar to pic beauty and others
- May not be the most

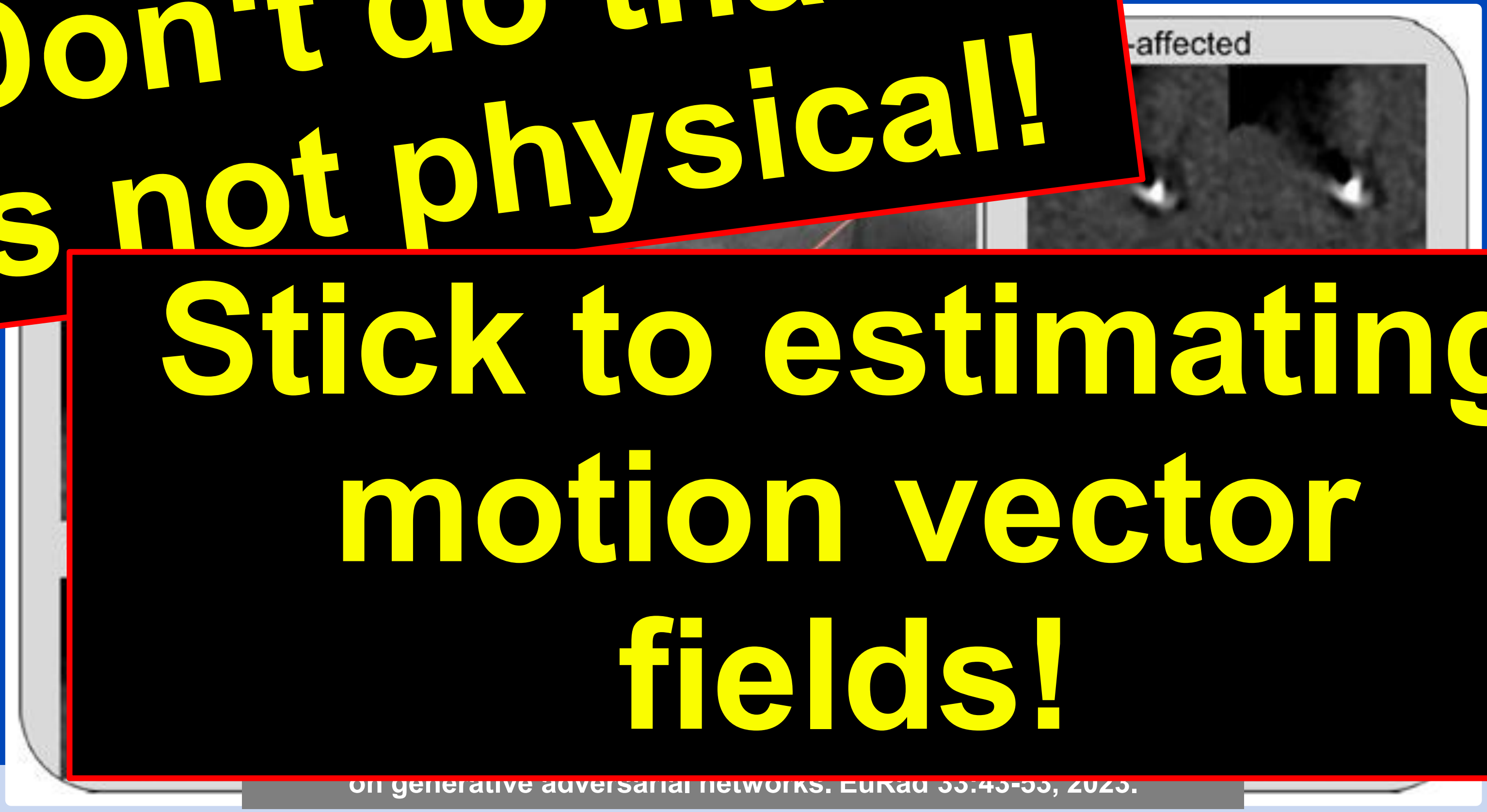

Don‘t do that!
It‘s not physical!

Stick to estimating motion vector fields!

on generative adversarial networks. EuRad 33:43-53, 2023.

Motion Compensation (MoCo)
Let the Voxels Move!

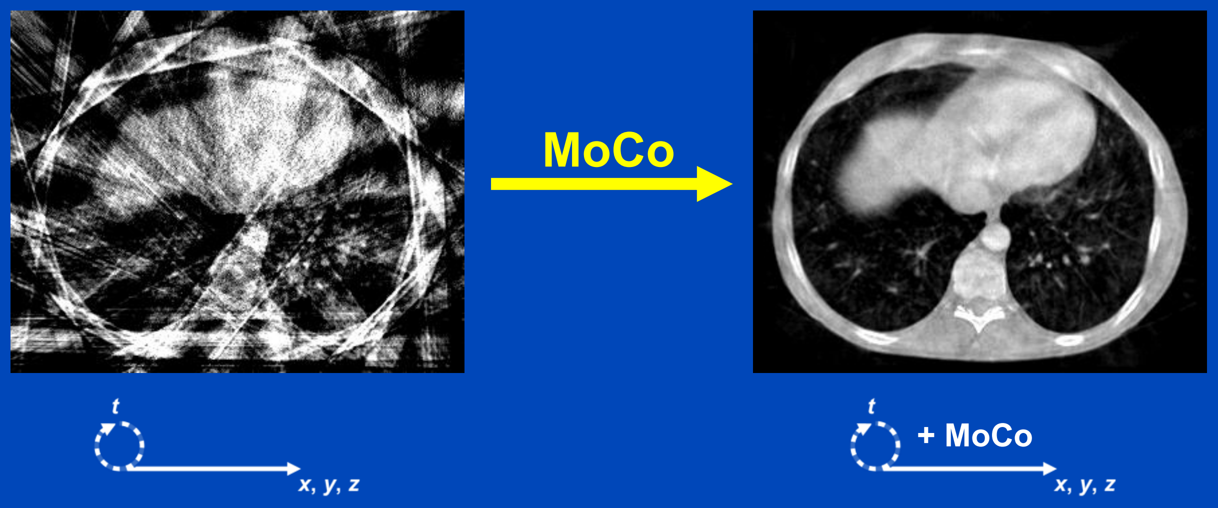

What is 4D?

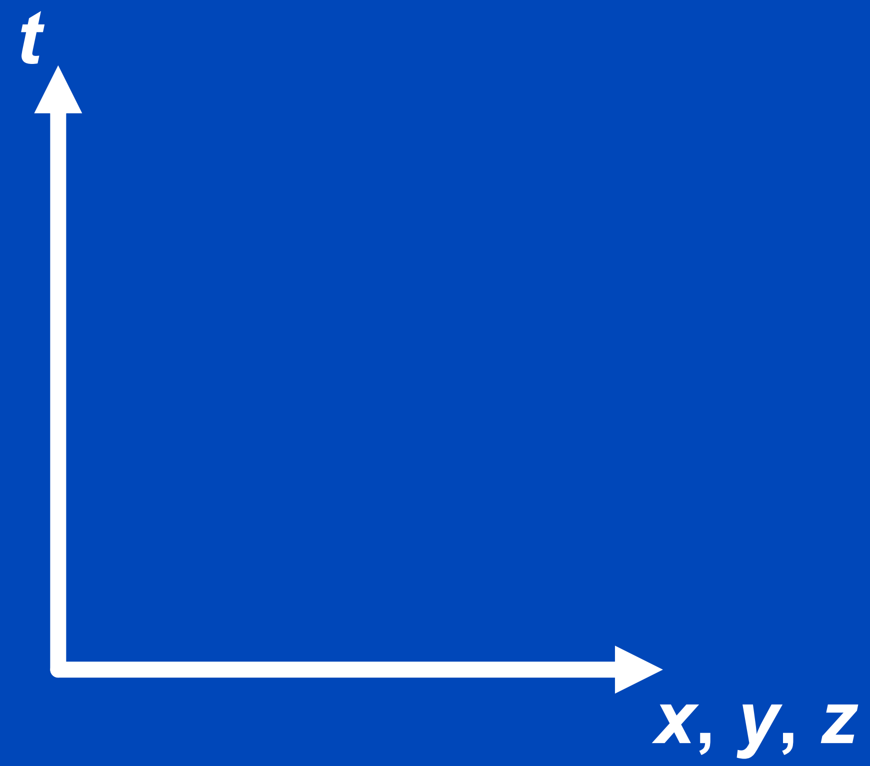

What is 4D?

Cyclic 4D

Assumes periodic motion

Needs breathing signal

Today's 4D CT and 4D CBCT

~ 500 ms temp. res.

~ 10 time points

Only before treatment

t

x, y, z

True 4D

t

Any kind of motion

No motion surrogate needed

Not available clinically

~ 10 ms temp. res.

> 500 time points

Also during treatment! → Tracking

x, y, z

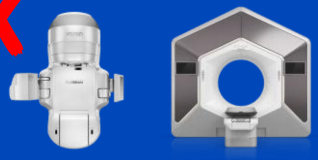

→ this presentation

Gating Fails on Irregular Breathing!

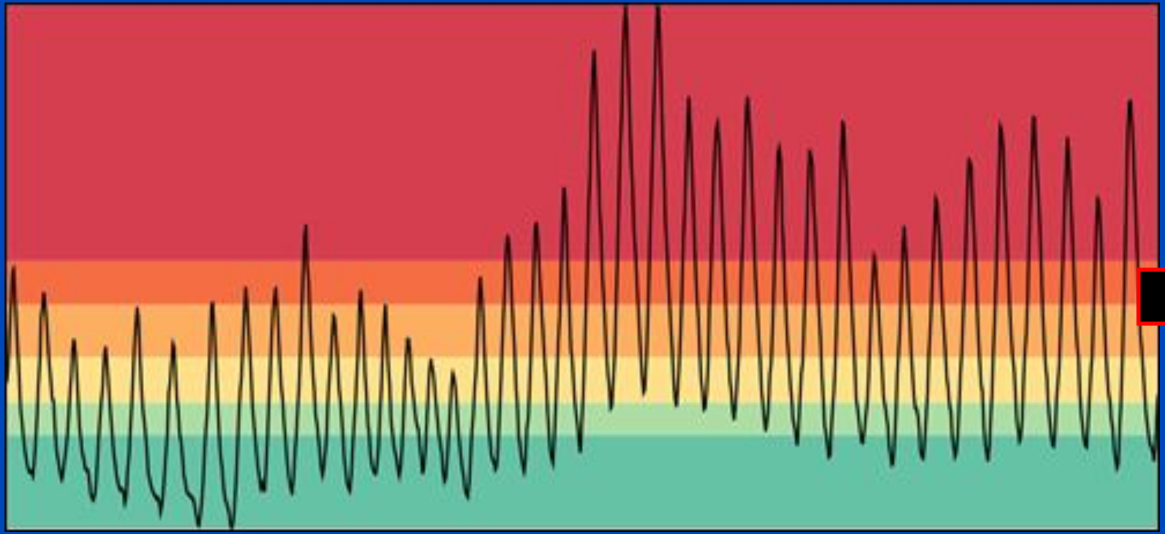

Gating = bad

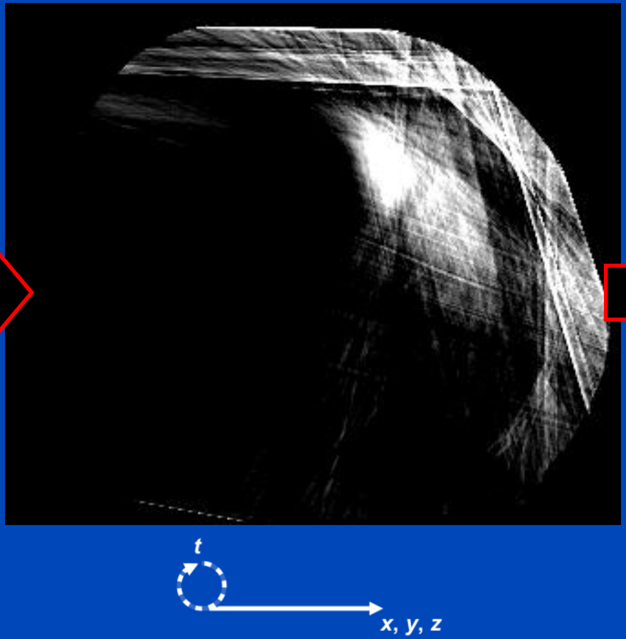

Gating + MoCo = still bad

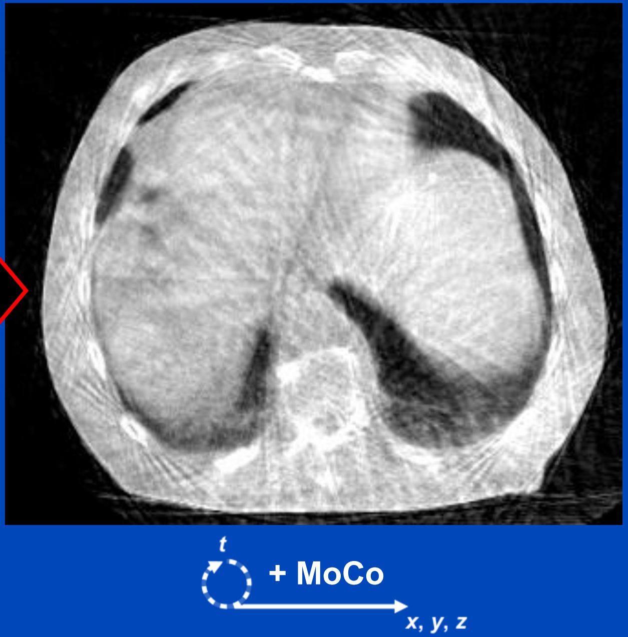

Single Angle Reconstructions (SARs)

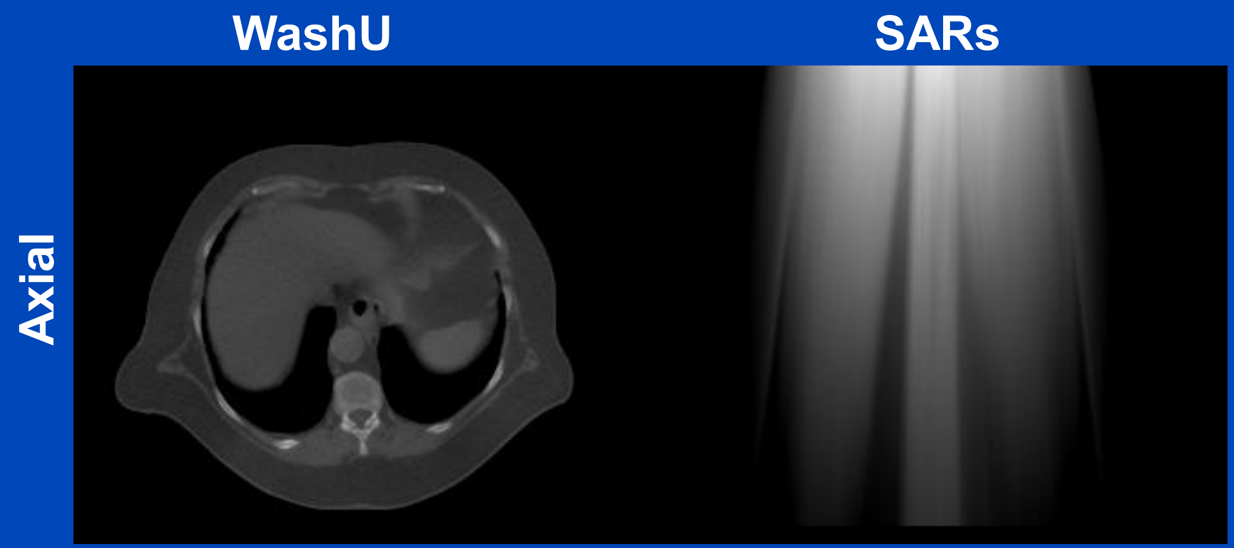

84 4D CT scans (no artifacts, high temporal resolution)

- 10 respiratory phases each (WashU/Colorado dataset)
- 10·10 combinations of phase *A* and *B* possible (including *A*=*B*)
- 84·10·10 displacement vector fields (DVFs) known
- 720 CBCT projections[1] simulated for each CT scan (each phase)
- 84·10·720·10·720 = 6.5 billion projection pairs with known DVF

[1]The actual projection numbers are between 420 and 900 and depend on the scan mode.

Training Workflow of Deep SAMoCo

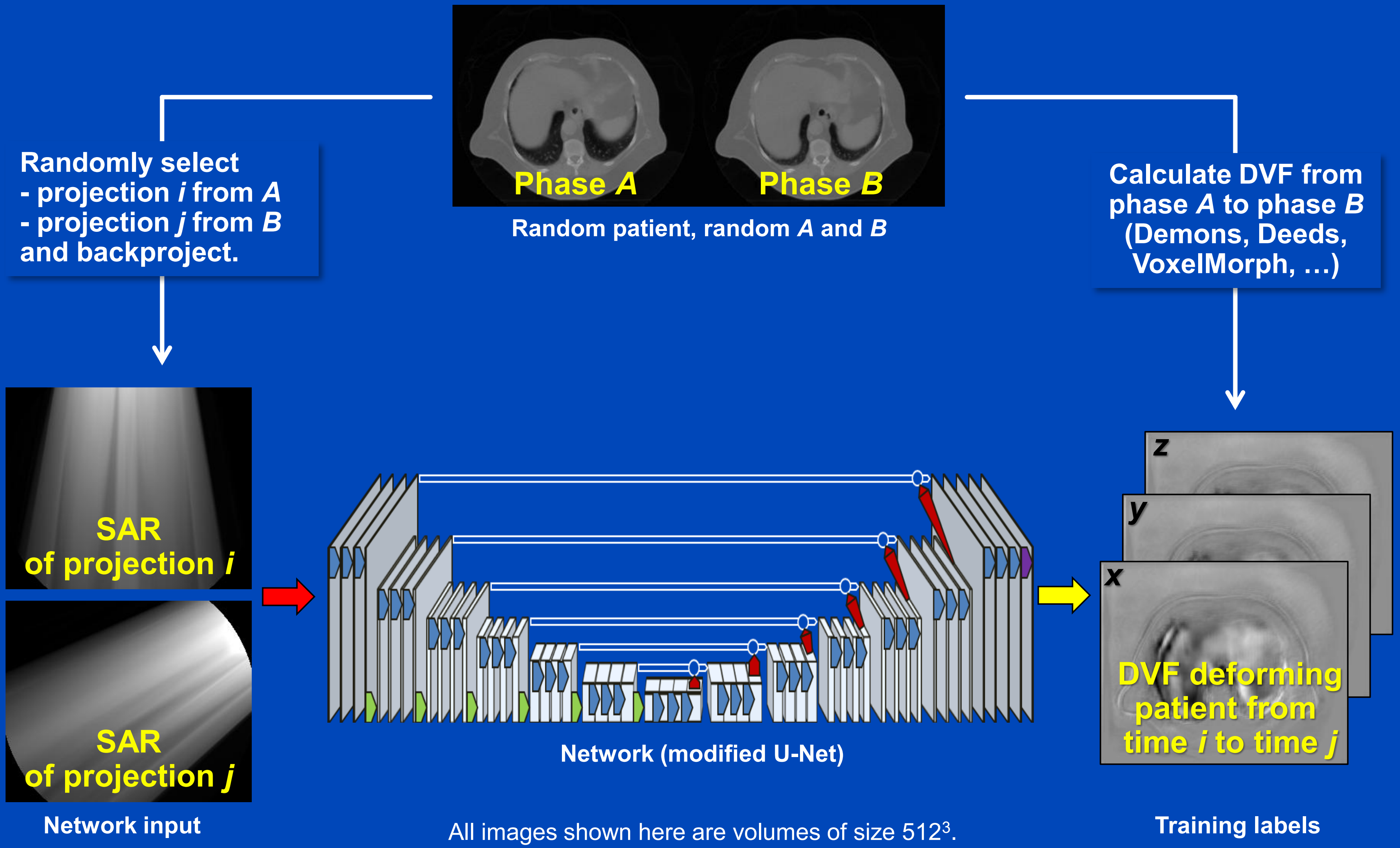

J. Maier, S. Sawall, M. Arheit, P. Paysan and M. Kachelrieß. Deep learning-based cone-beam CT motion compensation with single-view temporal resolution. Med. Phys. 52(7):e17911, July 2025.

Inference Workflow of Deep SAMoCo

- For a new patient
  - decide for the desired time point *j*, e.g. the one from 1 millisecond ago
  - for all $i \neq j$ get the DVFs pointing from *i* to *j* from the neural network
  - deform SARs for all $i \neq j$ into time point *j*
  - add all the volumes

For all $i \neq j$ do

Network input

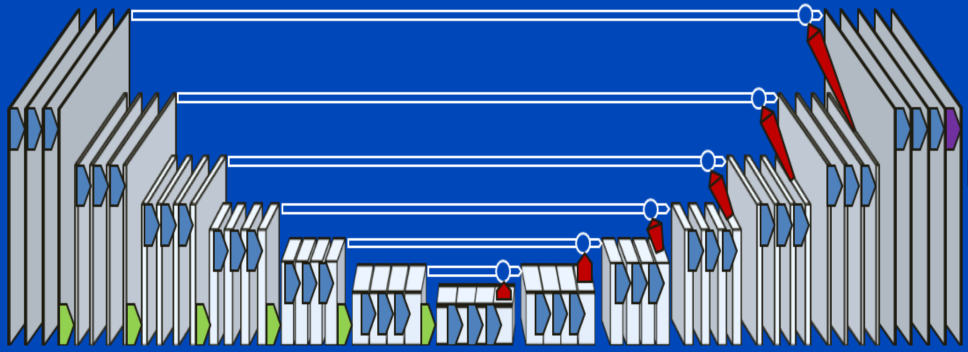

Network (modified U-Net)

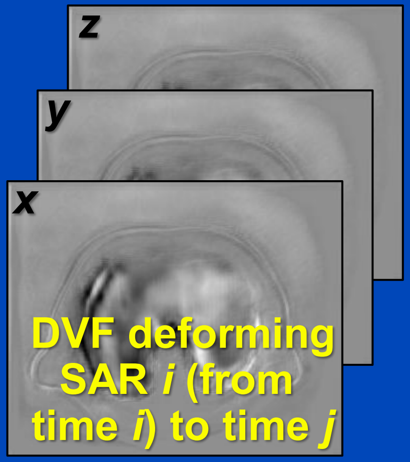

Network output

For the videos shown in the following, we did this for all 720 time points *j*

varian

J. Maier, S. Sawall, M. Arheit, P. Paysan and M. Kachelrieß. Deep learning-based cone-beam CT motion compensation with single-view temporal resolution. Med. Phys. 52(7):e17911, July 2025.

dkfz.

VUMC_4DThorax

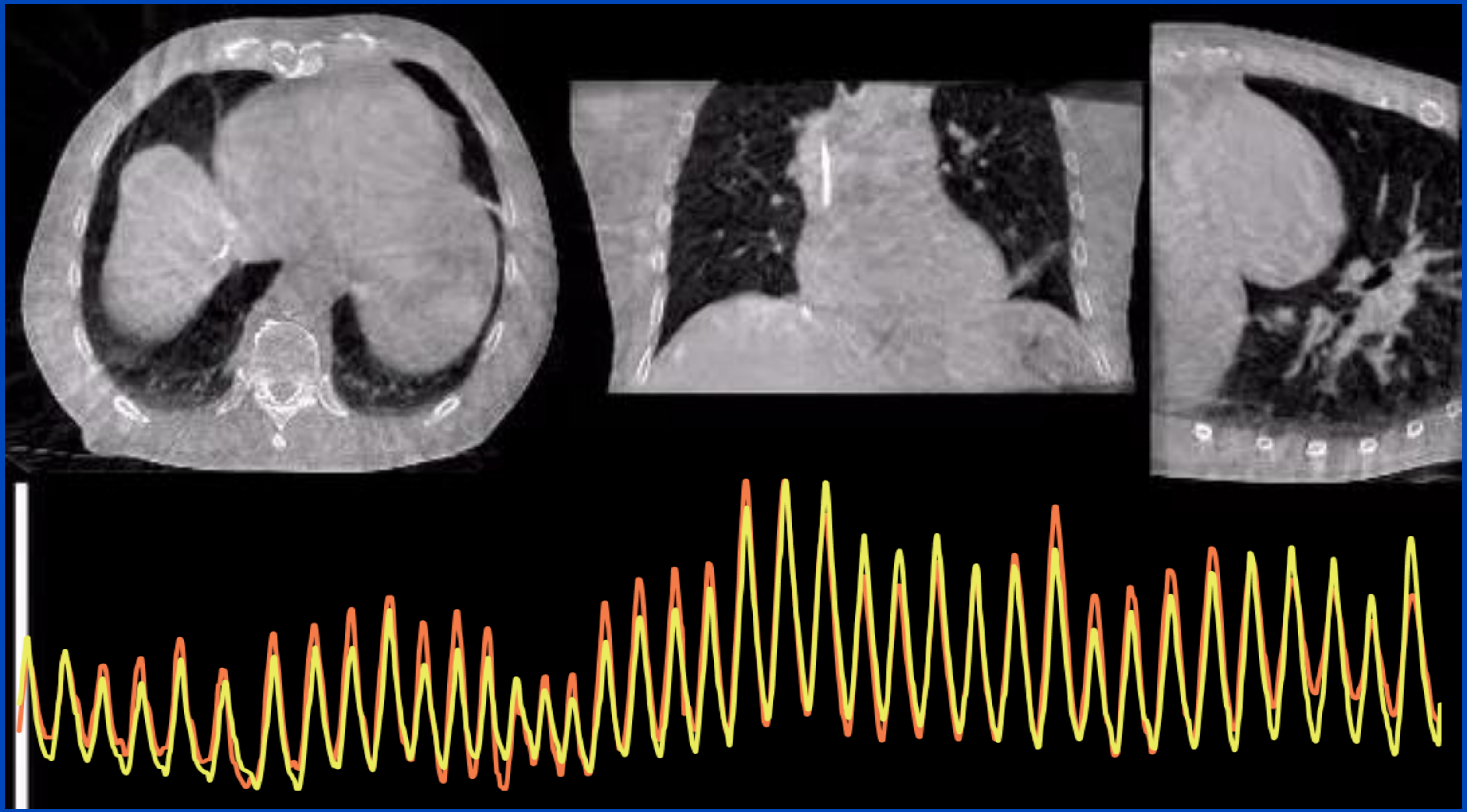

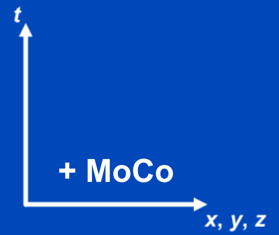

Red: RPM signal (external signal – not used for recon)
Yellow: Diaphragm motion (intrinsic signal – from PAMoCo recon)

MSK 1

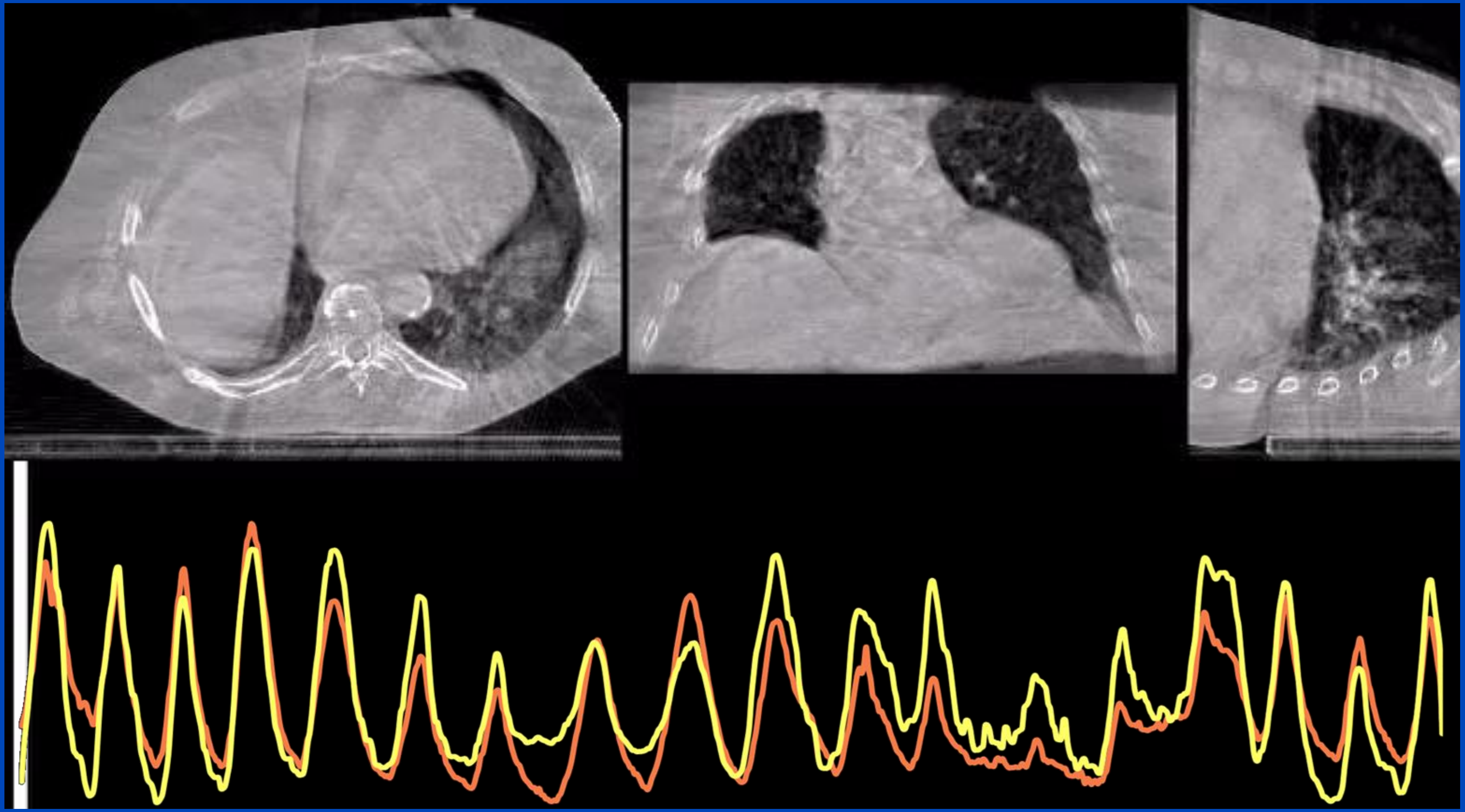

Red: RPM signal (external signal – not used for recon)
Yellow: Diaphragm motion (intrinsic signal – from PAMoCo recon)

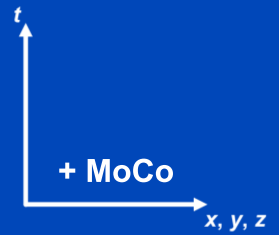

Thank You!

This presentation will soon be available at www.dkfz.de/ct.

Job opportunities through marc.kachelriess@dkfz.de or through DKFZ's international PhD or Postdoctoral Fellowship programs.

Parts of the reconstruction software were provided by RayConStruct® GmbH, Nürnberg, Germany.